INTERNATIONAL EFFICIENCY CHALLENGE ELECTRIC VEHICLE

TECHNICAL DESIGN REPORT

ÜNİVERSITY: ORTA DOĞU TEKNİK ÜNİVERSİTESİ

VEHICLE VE TEAM NAME: ALİZE / ODTÜ-TEK

ACADEMIC ADVISOR: PROF. DR. ERHAN İLHAN KONUKSEVEN

TEAM CAPTAIN: UFUK CAN KARATAŞ

VEHICLE TYPE: ☒ **ELEKTROMOBİL** ☐ **HİDROMOBİL**

Table of Contents

1. Vehicle Specifications Table

Feature	Unit	Value
Length	mm	3615
Width	mm	1564
Height	mm	1090
Chassis	material	Al 6082 T6
Shell	material	Carbon Fiber
The brake system	hydraulic disc, front, rear, hand brake	Front Hydraulic Disc
Motor	type	Steel-core Radial Flux
Motor driver	self-designed, ready-made product	Self-Designed
Motor power	kW	3.3 (peak)
Motor efficiency	%	93.8
Engine weight	kg	14.1
Battery	type	Li-ion
Battery pack nominal voltage	V	59,2
Battery pack capacity	Ah	36
Battery pack Maximum voltage	V	67,2
Battery pack energy	Wh	2131
Super capacitor	yes/no	No

2. Dynamic Driving Test

Dynamic driving test of Alize can be reached from the following YouTube link:

https://www.youtube.com/watch?v=LF85fhmVd0E

3. Domestic Components

1. Motor	**Mandatory for Electromobile/Hydromobile**	☒
2. Motor Driver	**Mandatory for Electromobile/Hydromobile**	☐
3. Battery Management System (BMS)	**Mandatory for Electromobile/Hydromobile**	☒
4. Embedded Rechargeing Unit	**Mandatory for Electromobile**	☒
5. Battery Packaging	**Optional**	☒
6. Electronic Differantial Application	**Optional**	☐
7. Vehicle Control Unit (VCU)	**Optional**	☒
8. Insulation Monitoring Device	**Optional**	☒
9. Steering System	**Optional**	☒
10. Door Mechanism	**Optional**	☒

4. Motor

Documents for our Motor Design: https://drive.google.com/file/d/1--nRgSBDrtJQintWaGpn3F8MTpicsJHK/view?usp=sharing

a. Design Calculations

We planned to produce a permanent magnet DC motor for our vehicle. Two different scenarios are analyzed to figure our motor's features. Calculations below are done by using Mathcad.

"Calculations"

*Scenario*1 – "While traveling at 50 kph, the vehicle has to have 0.3 m/s^2 acceleration."

"Mass" $m := 220\ kg$

"Density of air" $d := 1.225\ \frac{kg}{m^3}$

"Frontal surface area" $A := 1.223\ m^2$

"Drag coefficient" $Cd := 0.2$

"Coefficient of rolling res." $Crr := 0.008$

"Angle of slope" $\theta := 0\ deg$

"Acceleration" $a := 0.3\ \frac{m}{s^2}$

"Efficiency of motor-drive system" $eff := 0.9$

"Speed" $v := 50\ kph = 13.889\ \frac{m}{s}$

$r\_wheel := \frac{0.55}{2}\ m$ "Radius of the wheel"

"Weight" $W := m \cdot g = (2.157 \cdot 10^3)\ N$

$Ploss := 50\ W$ "Parasitic power loss due to bearings"

$Fdrag := \frac{1}{2} \cdot d \cdot Cd \cdot A \cdot v^2 = 28.9\ N$ "Force due to pressure drag"

$Frr := Crr \cdot W \cdot \cos(\theta) = 17.26\ N$ "Force due to rolling resistance"

$Fg := W \cdot \sin(\theta) = 0\ N$ "Force due to gravitational field"

$F\_a := m \cdot a = 66\ N$ "Force due to acceleration"

$Ftotal := Fg + Frr + Fdrag + F\_a = 112.16\ N$

$Ptotal := (Ftotal \cdot v) + Ploss = 1.608\ kW$

$Torque := Ftotal \cdot r\_wheel = 30.844\ N \cdot m$

$rpm := v \cdot \frac{1\ rev}{2 \cdot \pi \cdot r\_wheel} \cdot \frac{60\ s}{min} = 482.288\ rpm$

Scenario2 – "Vehicle^s speed should be 30 kph while climbing a hill with a slope %8.1 ."

"Mass"
$m := 220\ kg$

"Density of air"
$d := 1.225\ \frac{kg}{m^3}$

"Frontal surface area"
$A := 1.223\ m^2$

"Drag coefficient"
$Cd := 0.2$

"Coefficient of rolling res."
$Crr := 0.008$

"Angle of slope"
$\theta := 4.89\ deg$

"Acceleration"
$a := 0\ \frac{m}{s^2}$

"Efficiency of motor-drive system"
$eff := 0.9$

"Speed"
$v := 30\ kph = 8.333\ \frac{m}{s}$

$r\_wheel := \frac{0.55}{2}\ m$ "Radius of the wheel"

"Weight"
$W := m \cdot g = (2.157 \cdot 10^3)\ N$

$Ploss := 50\ W$ "Parasitic power loss due to bearings"

$Fdrag := \frac{1}{2} \cdot d \cdot Cd \cdot A \cdot v^2 = 10.404\ N$ "Force due to pressure drag"

$Frr := Crr \cdot W \cdot \cos(\theta) = 17.197\ N$ "Force due to rolling resistance"

$Fg := W \cdot \sin(\theta) = 183.909\ N$ "Force due to gravitational field"

$F\_a := m \cdot a = 0\ N$ "Force due to acceleration"

$Ftotal := Fg + Frr + Fdrag + F\_a = 211.51\ N$

$Ptotal := (Ftotal \cdot v) + Ploss = 1.813\ kW$

$Torque := Ftotal \cdot r\_wheel = 58.165\ N \cdot m$

$rpm := v \cdot \frac{1\ rev}{2 \cdot \pi \cdot r\_wheel} \cdot \frac{60\ s}{min} = 289.373\ rpm$

According to the calculations above, our motor's maximum speed and torque values are found to be 440 rpm (45kph) and 69 Nm respectively.

Design Parameters of the Motor

Our battery will consist of 16 cells with one potential 4.2V. In total, maximum battery voltage will be equal to 69.2V. However, by looking to the graph of potential change with respect to time, we used the nominal voltage value of the battery for the motor design, 59.2V.

Motor Fundamental Dimensions

"Torque value" "Number of Pole Pairs "

$TRV := 30 \frac{kN \cdot m}{m^3}$ $T := 0.069\ kN \cdot m$ $P := 21$ $\lambda := 1.5$

$D := \left(\frac{(T \cdot 4 \cdot 2 \cdot P)}{\pi \cdot TRV \cdot \pi \cdot \lambda} \right)^{\frac{1}{3}} = 296.63\ mm$ "Stator's outer diameter"

$L := \lambda \cdot \pi \cdot \frac{D}{2 \cdot P} = 33.282\ mm$ "Stator's thickness"

Stator and Rotor Dimensions

Stator and rotor dimensions calculated as;

$D_{outer} := 266\ mm$ "Stator Outer Dimension"

$h_o := 33\ mm$ "Stator Slot Height"

$h_b := 8\ mm$ "Stator Yoke height"

$D_{inner} := D_{outer} - 2 \cdot (h_o + h_b) = 184\ mm$ "Stator outer dimension"

$airgap := 1.5\ mm$ "Airgap"

$mag := 3\ mm$ "Magnet Thickness"

$h_{rb} := 11\ mm$ "Rotor Yoke Height"

$R_{inner} := D_{outer} + 2 \cdot airgap = 269\ mm$ "Rotor inner dimension"

$R_{outer} := R_{inner} + 2 \cdot (airgap + mag + h_{rb}) = 300\ mm$ "Rotor outer dimension"

Magnet Dimensions

In normal conditions, magnet thickness might be selected as 10 times the value of the airgap. In our design, airgap value is taken 1.5 mm considering the accuracy of the
machines while production and magnet thickness is selected to be 3 mm after the magnetic design.

Winding Scheme

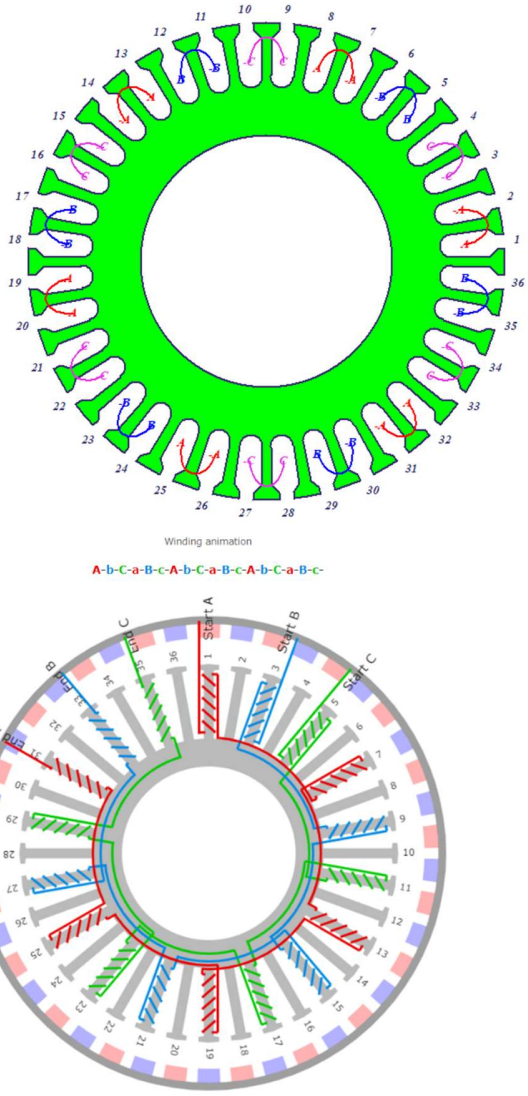

Optimization

During the analysis period, dimensions were being changed to find the case with lowest consumption and highest efficiency value. Because of this, some dimensions such as magnet thickness, stator or rotor dimensions are optimized by the “Optimetrics” option of Ansys Maxwell.

b. Magnetic Analysis Studies

The magnetic design of the motor and the necessary analysis are done with Ansys Maxwell finite element tool.

To increase the efficiency, we tried to keep the core loss and copper loss low. It is known that core loss increases with high flux density and frequency, on the other hand, copper loss increases with the rate of current passing and the resistance of the wire used. Our goal is keeping flux density and frequency low and decreasing the current rate. Our design's frequency is 100-150 Hz in when rotating during the race which is small for an efficient motor. Flux density is calculated via Maxwell and kept lower than 1.7 Teslas in normal conditions.

Finite Element Analysis (FEA) results for our motor at 480 rpm speed is given in following figure:

Figure 3. Mechanical Output Power vs Time

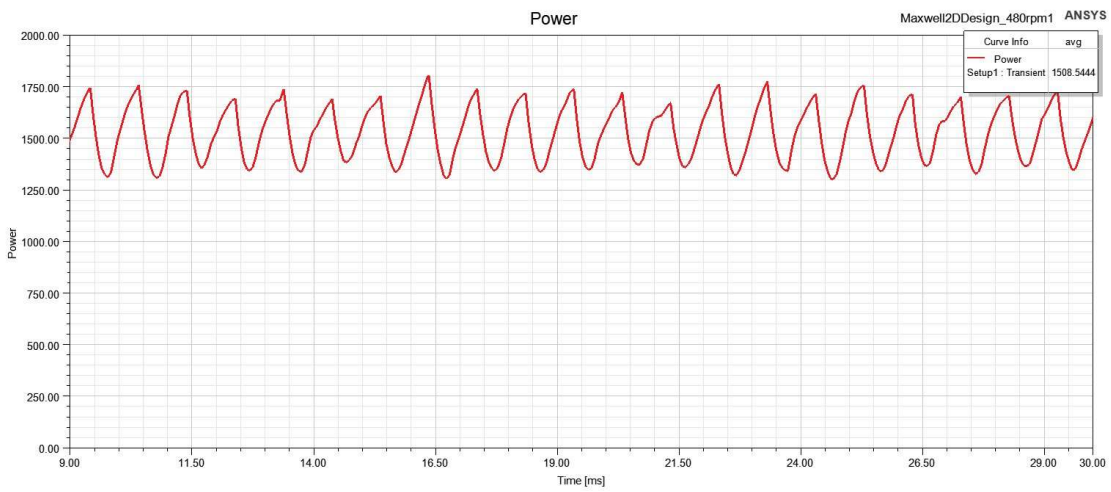

Figure 4. Nominal Phase Currents vs. Time

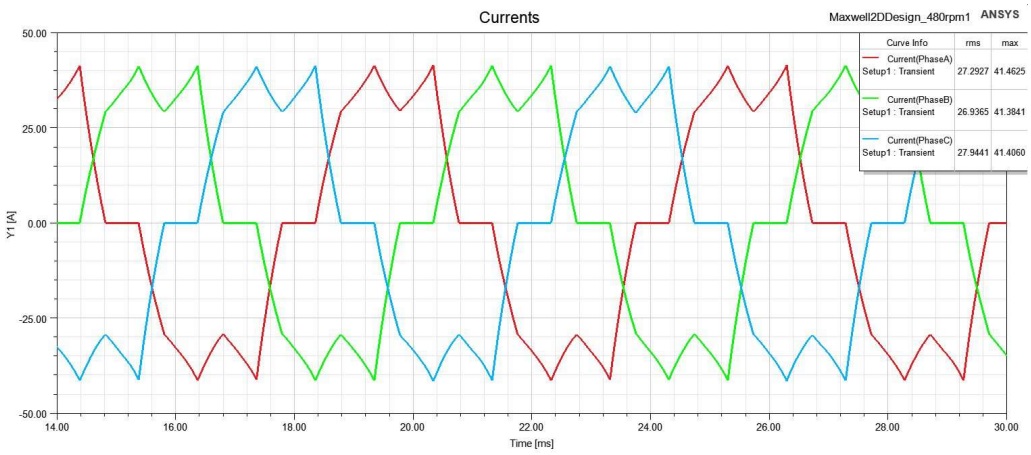

Figure 5. The efficiency of the motor vs Time

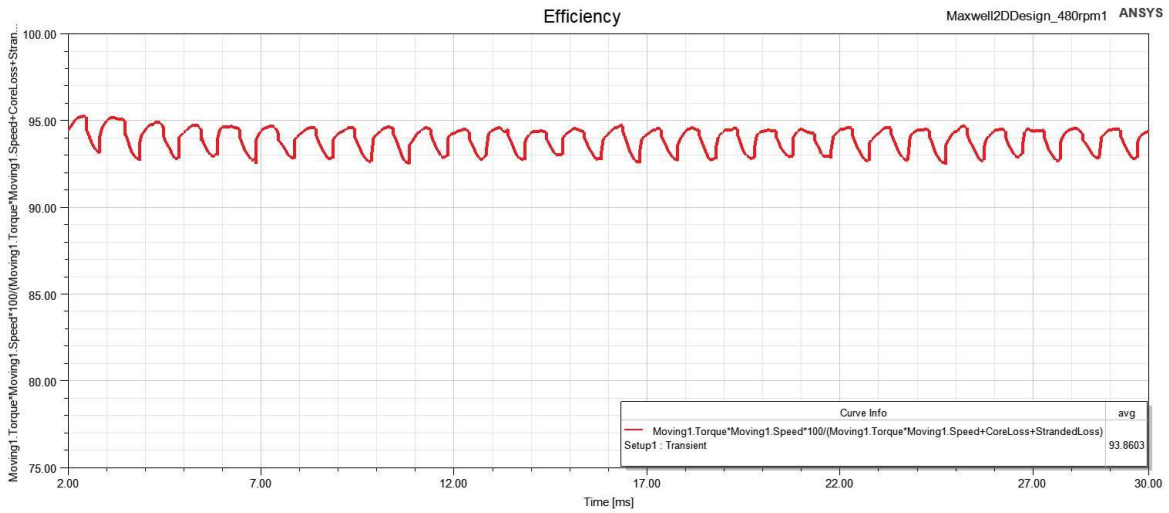

Figure 6. Flux Density-Maxwell 2D Analysis

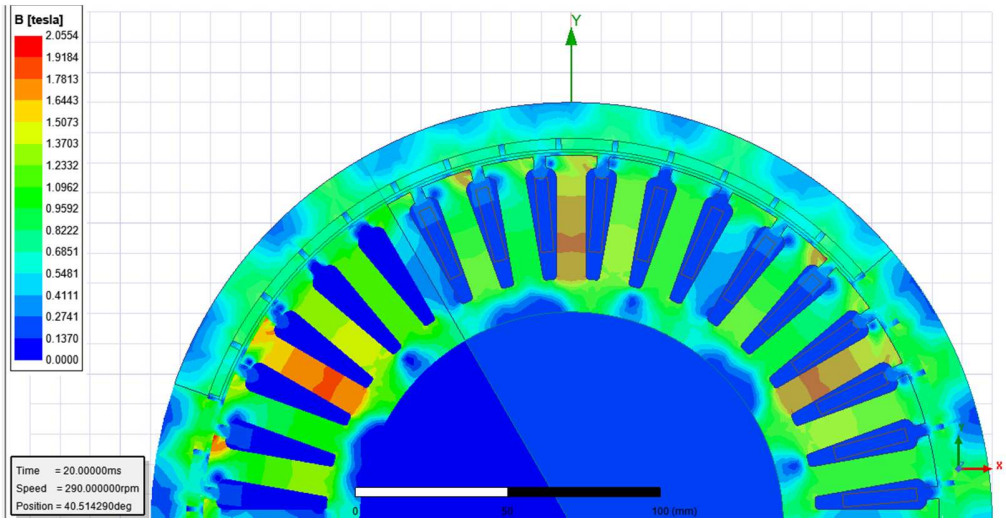

Figure 5 shows that our design has a high efficiency rate of 93.8% which is difficult to achieve.

c. Mechanical Design and Analysis Studies

Mechanical analysis studies are performed on SolidWorks 2020 Simulation. The factor of safety of the mechanical parts is given below. The factor of safety is kept close to 2 to both be safe and not to use excessive material and, as a result, reducing mass and rotational inertia. Thrust is created by the torque exerted on the wheel and carried by the case. Thus, case and holder are analyzed under maximum torsional load, which is 60 Nm. Case and shaft also carry the load that comes from the ground. That is why we used “Remote Load” command in SolidWorks Simulation to have a better analysis.

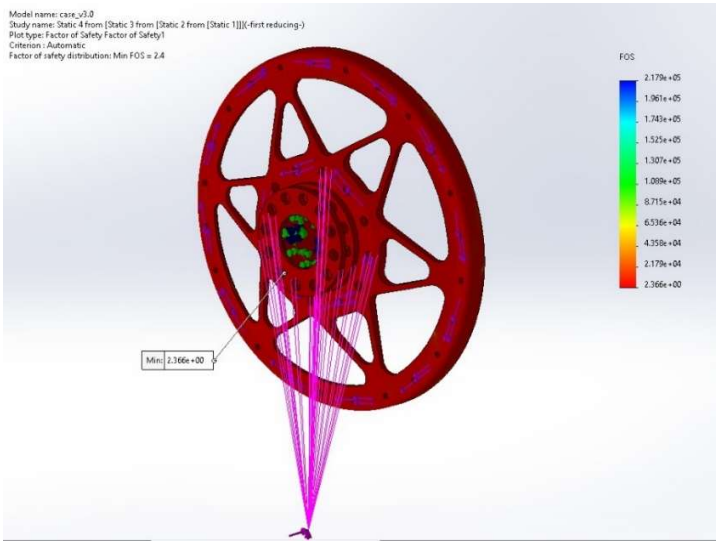

Figure 7. Factor of Safety of the Motor Case

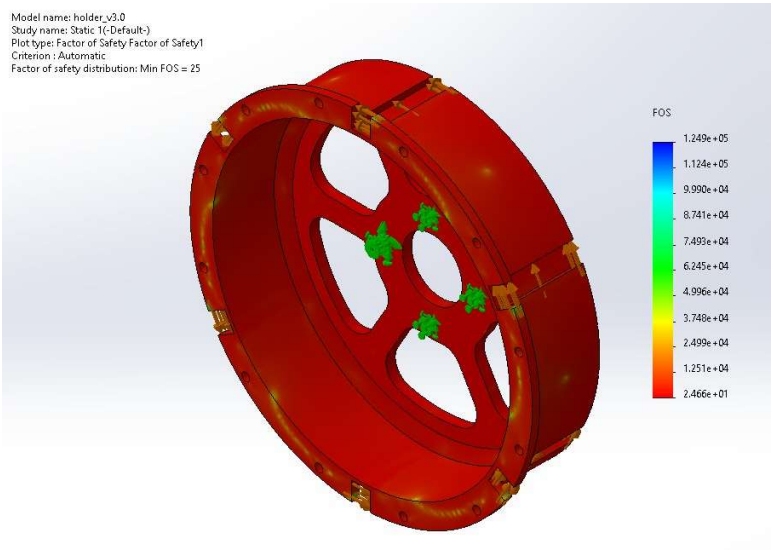

Figure 8. Factor of Safety of the Holder

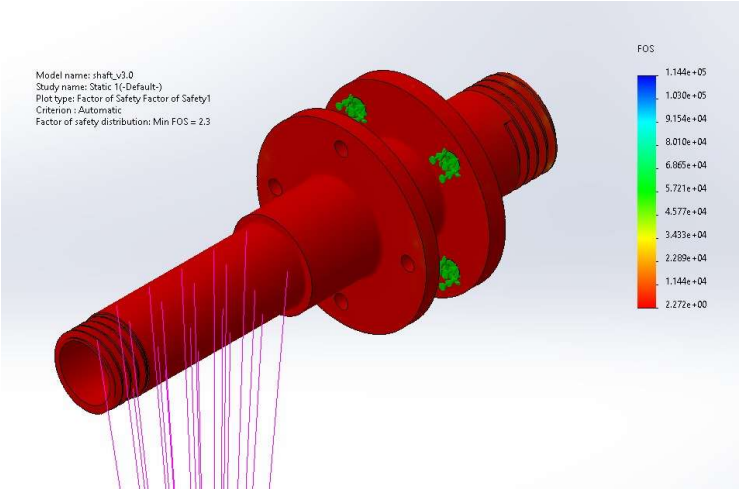

Figure 9. Factor of Safety of the Shaft

d. Thermal Analysis Studies

After finishing the mechanical design, thermal analysis is done to see the thermal behavior of the motor while operating. SolidWorks 2020 Flow Simulation, a CFD application is used for the analysis. Figure 7 is the thermal model of our motor assembly.

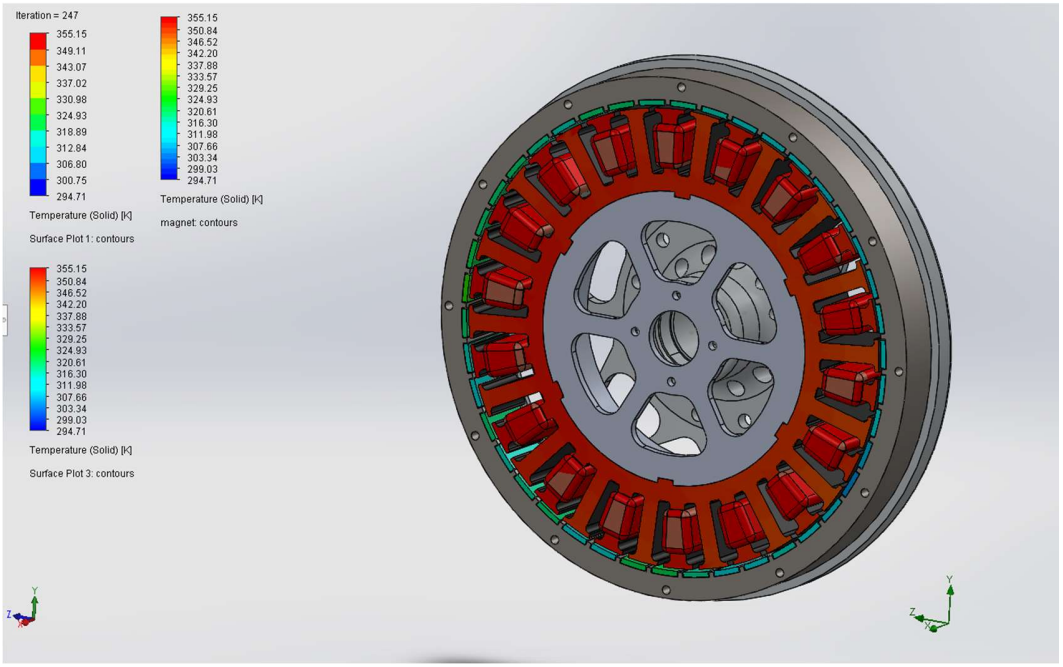

Figure 7. Thermal Model of the motor

Before making the thermal analysis, the temperature of the magnets was very important since their magnetic characteristics are lost in temperatures higher than 80 °C. According to the analysis results, our magnets will be heated up to 333K (60 °C) which is convenient for us. The temperature of the coils was also crucial because the melting temperature of the coating (300 °C) cannot be exceeded. In the analysis, it is seen that the temperature at the coils is 82°C.

Cooling System	Current density A/mm²	Cooling efficiency	Complexity	Energy cost
Free convection	1.5 – 5	Low	Simple	None
Forced convection	5 – 10	Medium	Medium	Low
Liquid cooling	10 – 30	High	Complex	High

According to these results and the current density data that comes from Ansys Maxwell, an optimal way of cooling is chosen. Maximum current density is approximately 5A/mm^2 and according to the chart of EOMYS Engineering (2019), free air convection is an efficient way of cooling.

e. Production Studies

After the completion of the computer analysis, the production part has started. It is possible to list our production studies in 6 stages.

1. Production of the parts designed by machining (except stator)
2. Cutting the siliceous sheets metal
3. Unifying the sheets and forming the stator
4. Winding the wire around the stator

We used press tape to prevent short circuit in the stator.

5. Placing the magnets in the rotor

Strong glues are used to fix the magnets.

6. Placing the thermal and hall effect sensors in the motor and checking the results

After those stages, the motor is assembled, and our production studies are terminated.

Technical drawings are all shared in the .zip file. Link is given below again:
https://drive.google.com/file/d/1--nRgSBDrtJQintWaGpn3F8MTpicsJHK/view?usp=sharing

f. Motor Tests and Results and Efficiency

In order to precisely measure the efficiency, one needs wattmeter to measure input power and torquemeter to measure output power. Since we don't have either of them, we could not make any experiment in terms of efficiency.

		Previous Design	New Design
Motor Type	:	BLDC	BLDC
Motor Phase Voltage	:	44.4 V	59.2 V
Motor Power	:	1.8 kW	2.1 kW
Motor Speed	:	440 rpm	480 rpm
Motor Dimensions	:	280mm*280mm*36mm	300mm*300mm*39mm
Motor Weight	:	10 kg	14.1 kg
Motor Efficiency	:	89.5 %	93.8 %
Motor Main Dimensions	:	D=263 mm(stator diameter) L=32mm(stator thickness)	D=296 mm(stator diameter) L=33 mm(stator thickness)
Stator Dimensions	:	Ø 244 mm	Ø 264 mm
Rotor Dimensions	:	Ø 280 mm	Ø 300 mm
Winding Scheme	:	Star	Star
Motor Optimization	:	Ansys Maxwell 2D	Ansys Maxwell 2D
Magnetic Design and Analysis Model	:	Ansys Maxwell 2D	Ansys Maxwell 2D
Thermal Design and Analysis Model	:	SolidWorks 2020 Flow Simulation	SolidWorks 2020 Flow Simulation
Mechanical Design and Analysis Model	:	SolidWorks and Ansys Workbench	SolidWorks and Ansys Workbench
Motor Test Methods and Results	:	-	-

5. Motor Driver

Motor driver is bought from Kelly Controllers, Inc. It generates sinusodial waves which complies with winding schematics of the motor. Also, the motor driver has seals to operate safely in water and dust.

6. Battery Management System (BMS)

		Previous Design	New Design
Battery Pack Design	:	Domestic	Domestic
Output Voltage	:	Max:50.4V, Nominal:44.4V	Max:67.2V, Nominal 59.2V
Output Current	:	Peak 360A, Continuous 120A	Peak 360A, Continuous 120A
Balance Method	:	Passive	Passive
Circiut Design Type	:	Mixed Type	Mixed Type
SOC Estimation Algorithm	:	Data Acquisition	Data Acquisition
Control Algorithm	:	Passive Balancing	Passive Balancing
Domestic or Imported	:	Domestic	Domestic

We chose the bq76pl455 IC because we wanted to develop a circuit that was inexpensive, easy to manufacture, and debug. We use the IC's datasheet and design instructions to create the circuit. TI provided a wealth of information regarding IC in those references. The balancing part of the circuit is the initial part of our design. TI utilized a 2v7002 N-Channel FET in the datasheet for the BQ76PL455, thus we selected a 2n7002 with a maximum balancing current of 35mA. In addition, our measuring pins incorporate an RC low pass filter for more precise data. The filter's cut-off frequency is 159Hz.

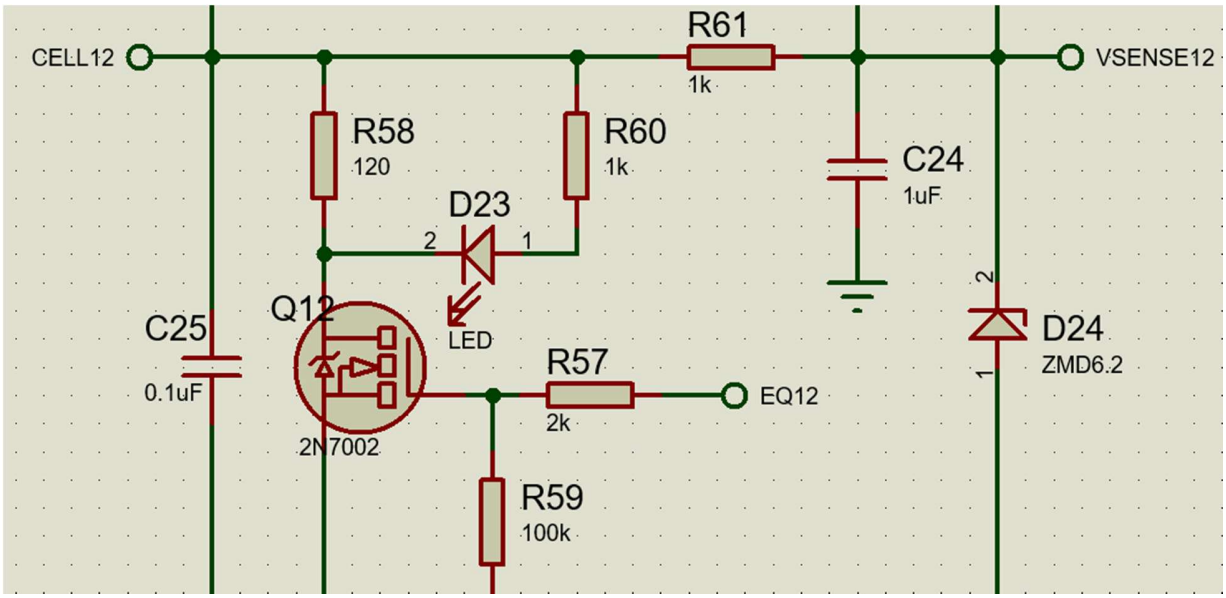

Figure 6.1: Balance circuit of one cell

The block in the Figure 6.1 is the balancing block of our circuit and we have it for every cell. It is a passive balancing circuit.

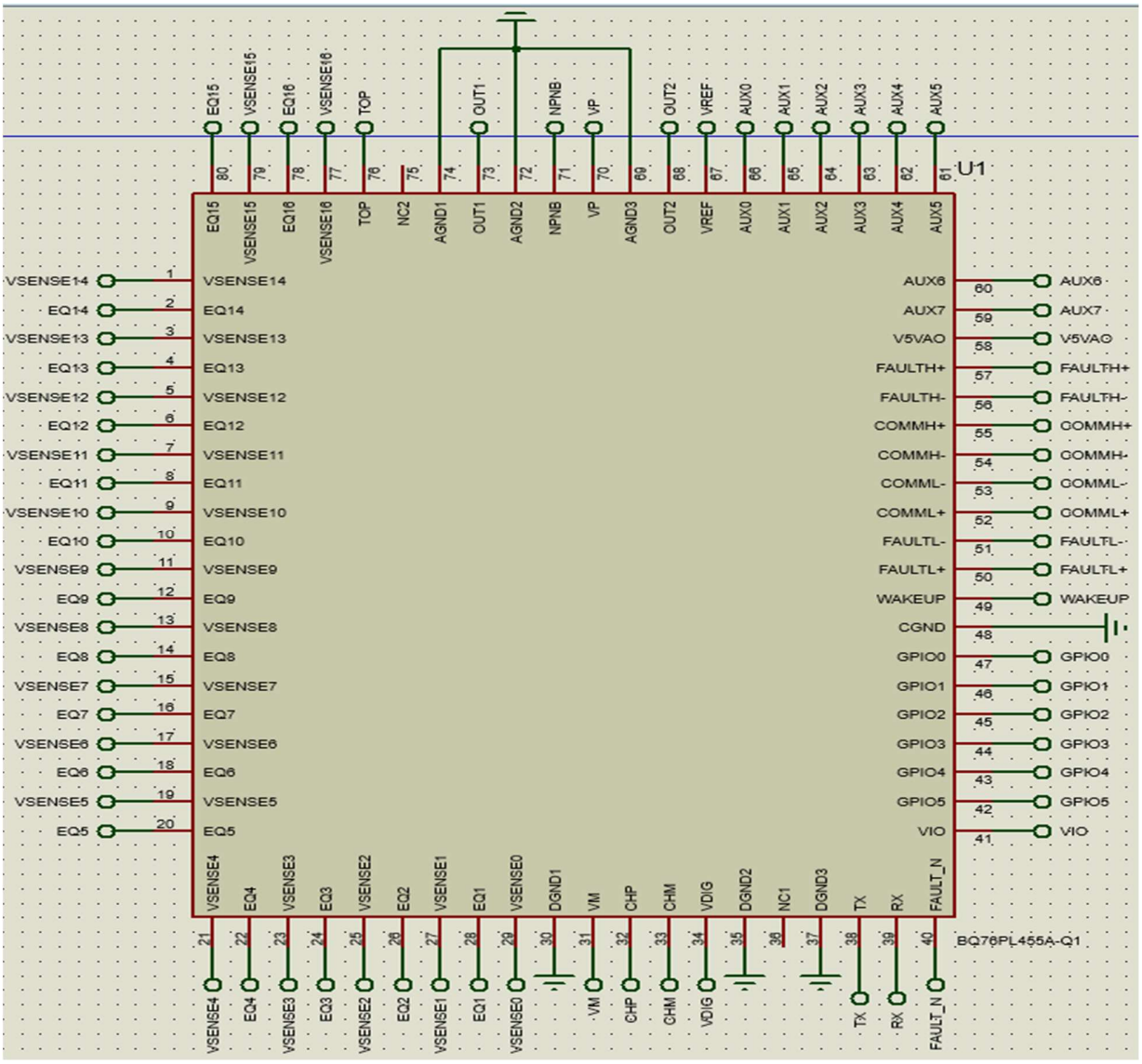

Figure 6.2: Main IC of our BMS

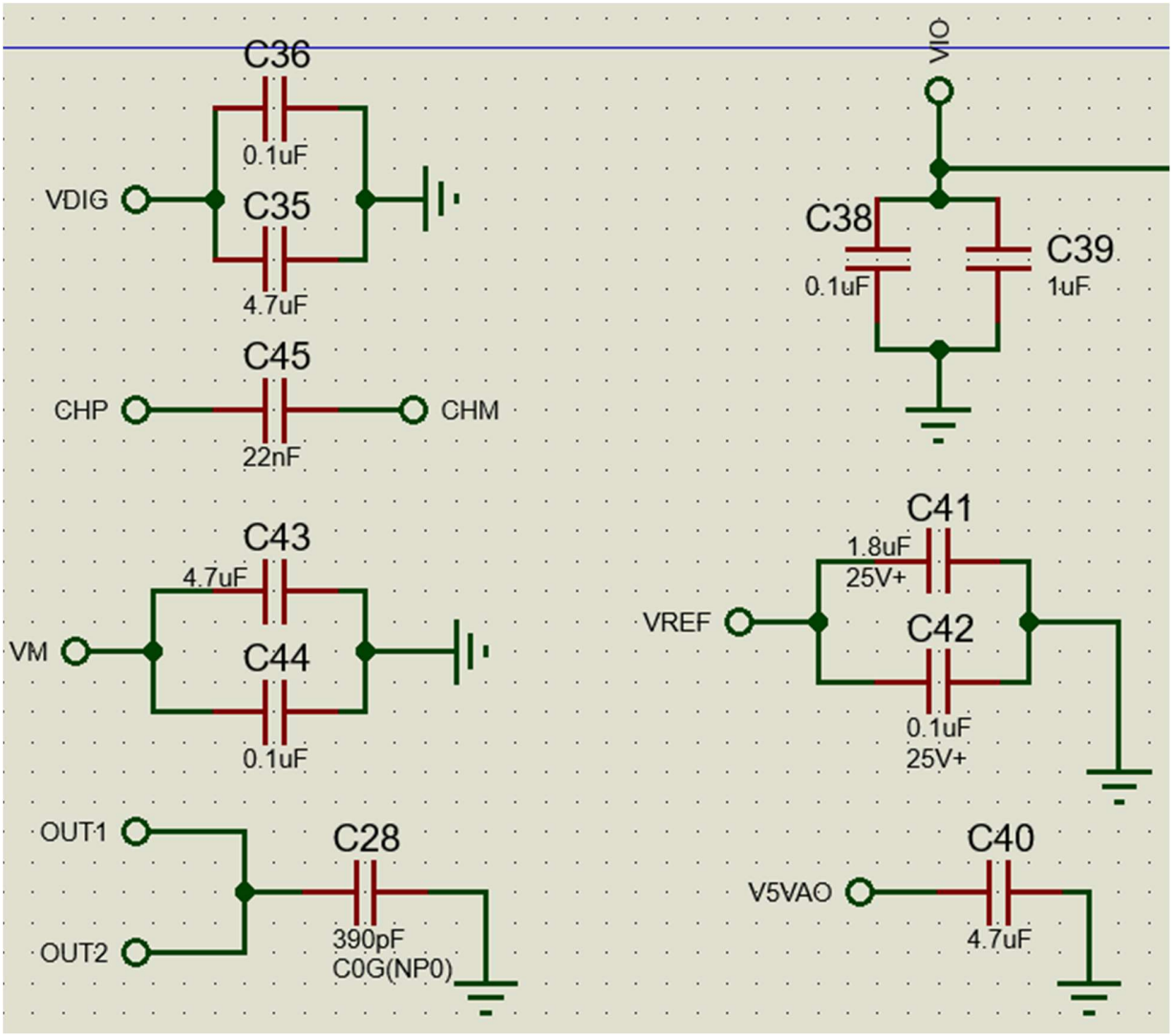

Figure 6.3: Capacitors

Figure 6.3 shows decoupling capacitors as well as a charge pump capacitor for driving gates. It's critical to use the proper capacitors in your design because TI won't guarantee the IC's functionality if you don't.

We opted to segregate our MCU from the BMS in order to create a really secure design (since all other circuits are supplied with an isolated converter, all other components are isolated from battery). Furthermore, communication across circuits might be exceedingly expensive if the isolation is not broken. We segregated our MCU and BMS IC so that we could use any communication protocol we wanted. Our BMS IC communicates via UART and CAN; to isolate UART, we require a 1/1 isolator; however, to control IC wake-

up and Fault pin, we need a 2/2 isolator. We chose ISO7742, a 2/2 digital isolator, because of its low cost and great performance.

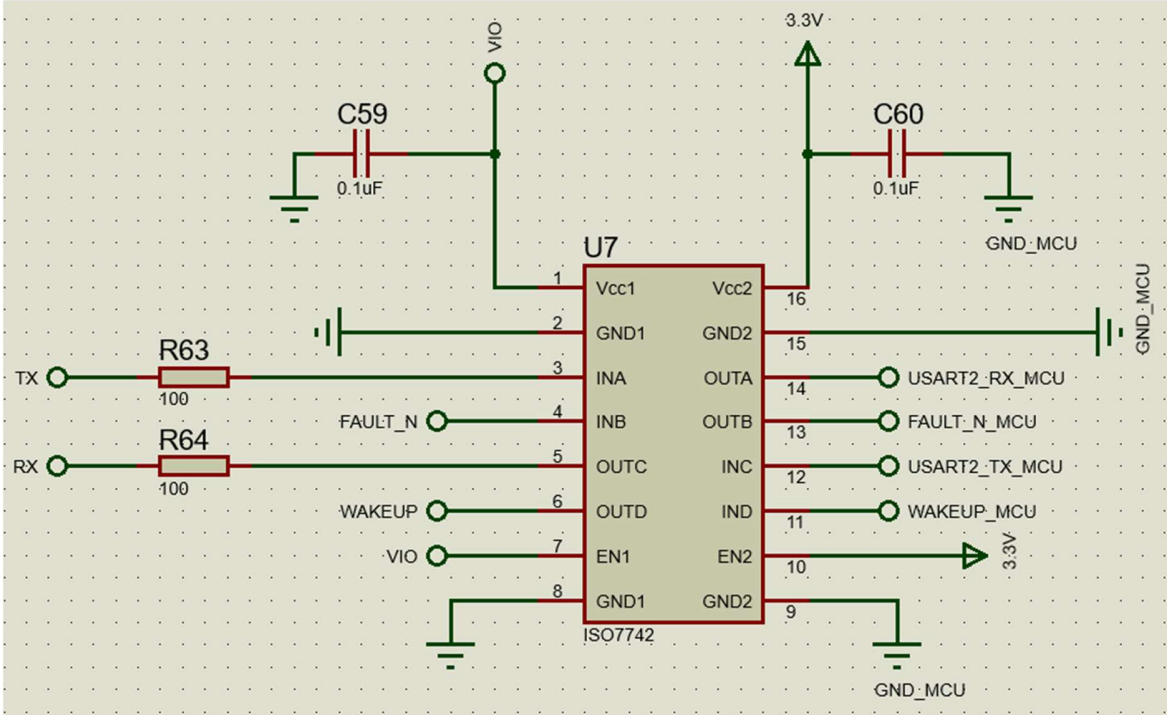

Figure 6.4: Isolation circuit

An isolated dc-dc converter is required to achieve isolation. We intend to use isolated dc-dc converters from Mean Well. It's tiny and efficient, and it doesn't need any external cooling.

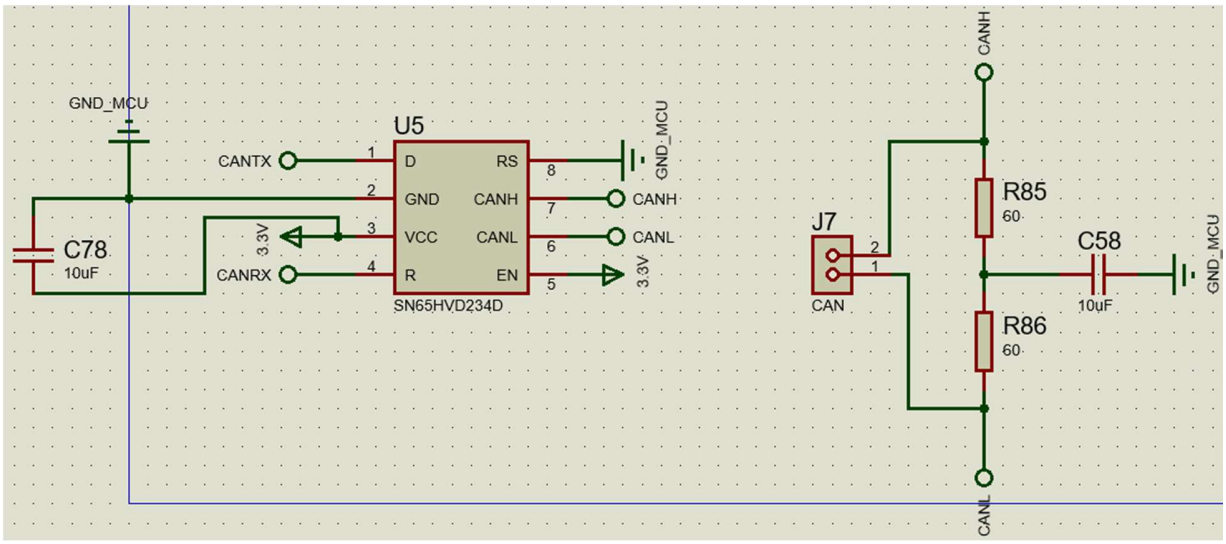

Figure 6.5: CAN communication circuit

We produced a schematic of the MCU portion after measuring, balancing, and isolating it. We chose the STM32F103 as our MCU since it has a large number of GPIOs and supports a variety of communication protocols.

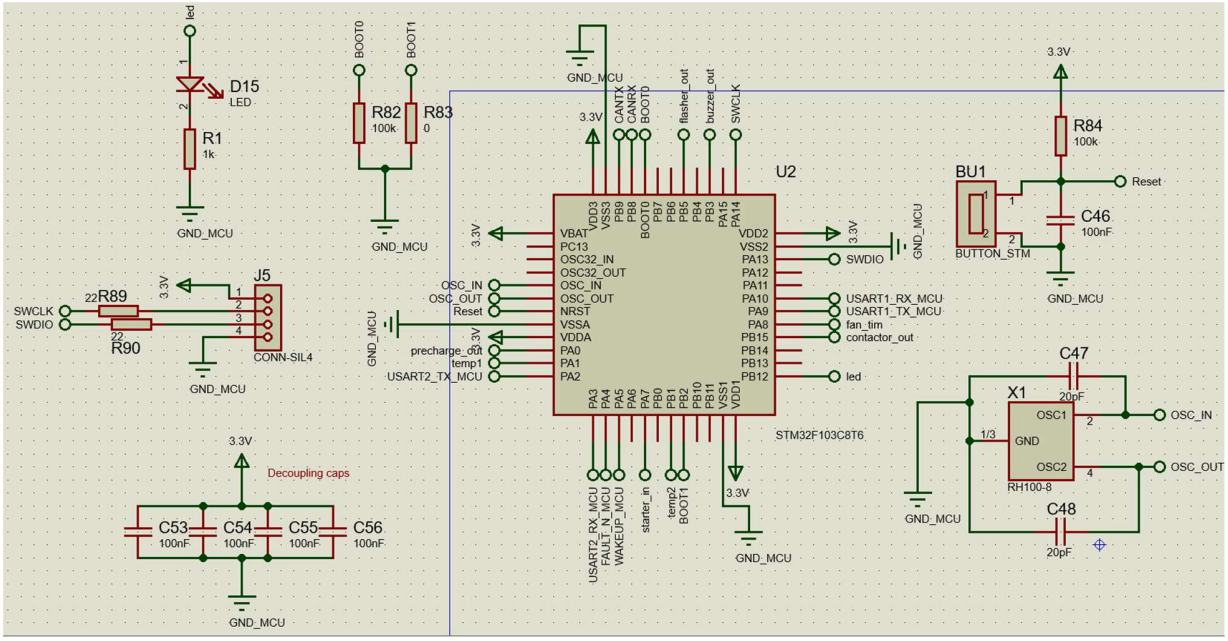

Figure 6.6: STM32F103 schematic

Temperature is measured using MCU ADCs. We also set up timer 1 to generate PWM, which controls the speed of the fan based on the temperature. Furthermore, the MCU is in charge of the buzzer, the start button, the precharge circuit, and the contactor. Emergency switches are not digitally controlled to ensure that they continue to function even if the MCU or any other component fails.

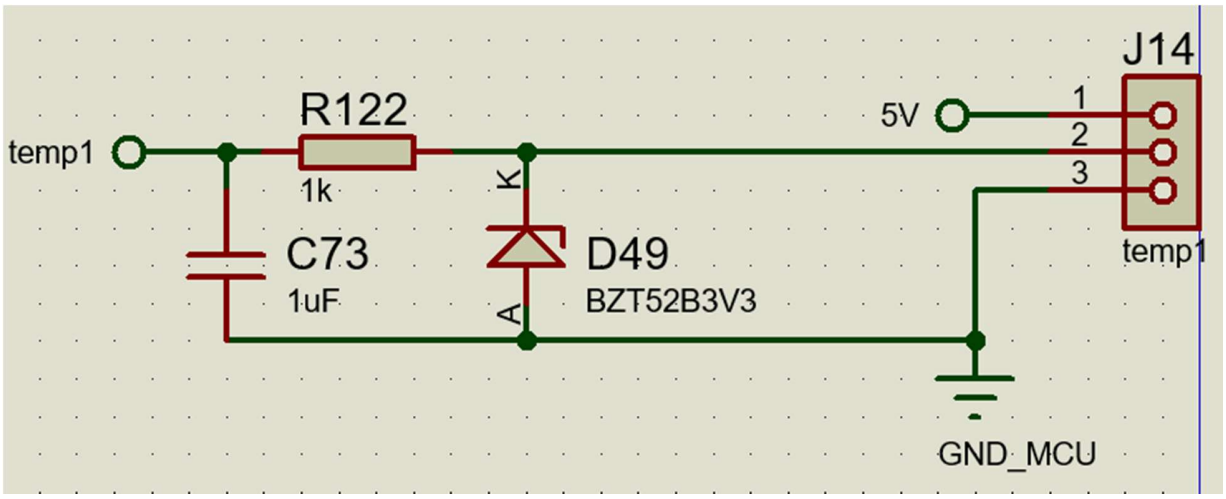

Figure 6.7: ADC measurement block

In our ADC channels, we add several RC low pass filters and protection diodes, as seen in Figure 6.7. Our MCU does all of the temperature control work; it compares all of the temperature sensors and then accepts the higher temperature as the pack temperature.

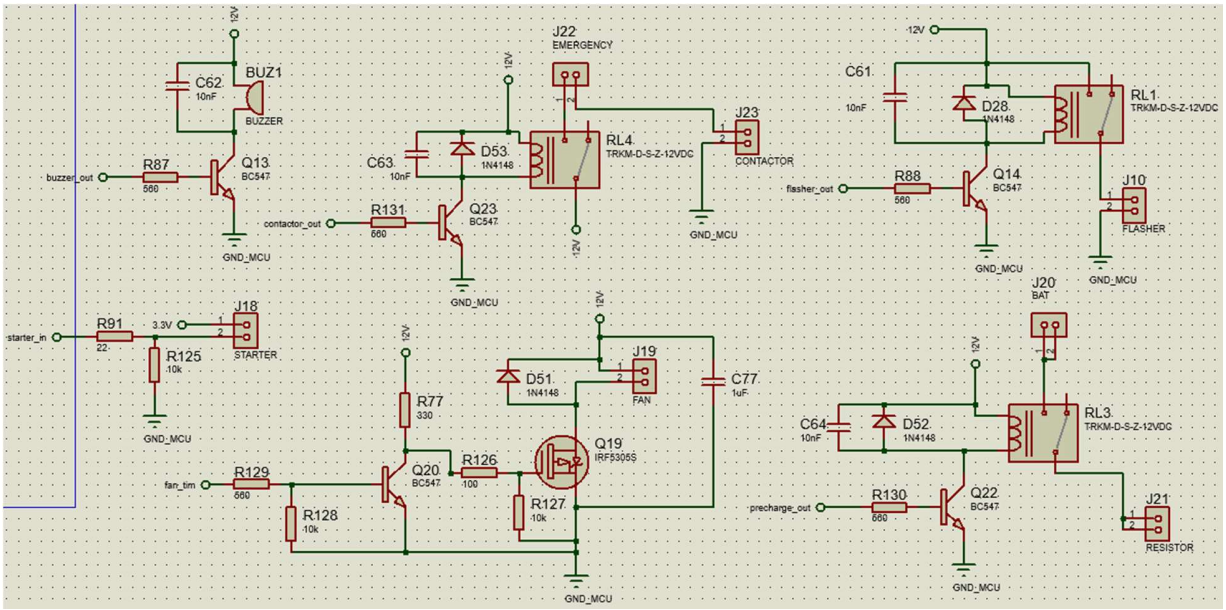

Figure 6.8: Control of buzzer, starter button, contactor, fan, flasher and precharge

We used relays to make precharge and regulate the contactor and flasher, as shown in Figure 6.8. Furthermore, our emergency switches have the ability to regulate the contactor. The fan speed can be controlled by the MCU, however if there is no signal in the TIM1 CH1, the fans will spin at maximum speed.

We began designing the PCB after the schematic was completed. Our BMS has isolated two parts, one of the is the battery monitoring part and the other part do the control. The boards' dimensions are 164mm*118mm, and it is two-layer.

Our BMS's balancing method is passive balancing. We chose that strategy since it is less expensive and simple to apply. Furthermore, with a battery pack with those energies, using an active balancing BMS has a number of drawbacks, including cost, circuit size, and significantly more difficult testing.

The balancing control is handled entirely by the BQ76PL455 IC. Its registers are programmed to set the OVP and UVP. The IC examines all of the voltages, compares them internally, and discharges any cell with a higher voltage than the others.

First, to test the circuit, we made a resistor ladder instead of connecting battery itself. There is a GUI for BQ76 and we see the cell voltages on that.

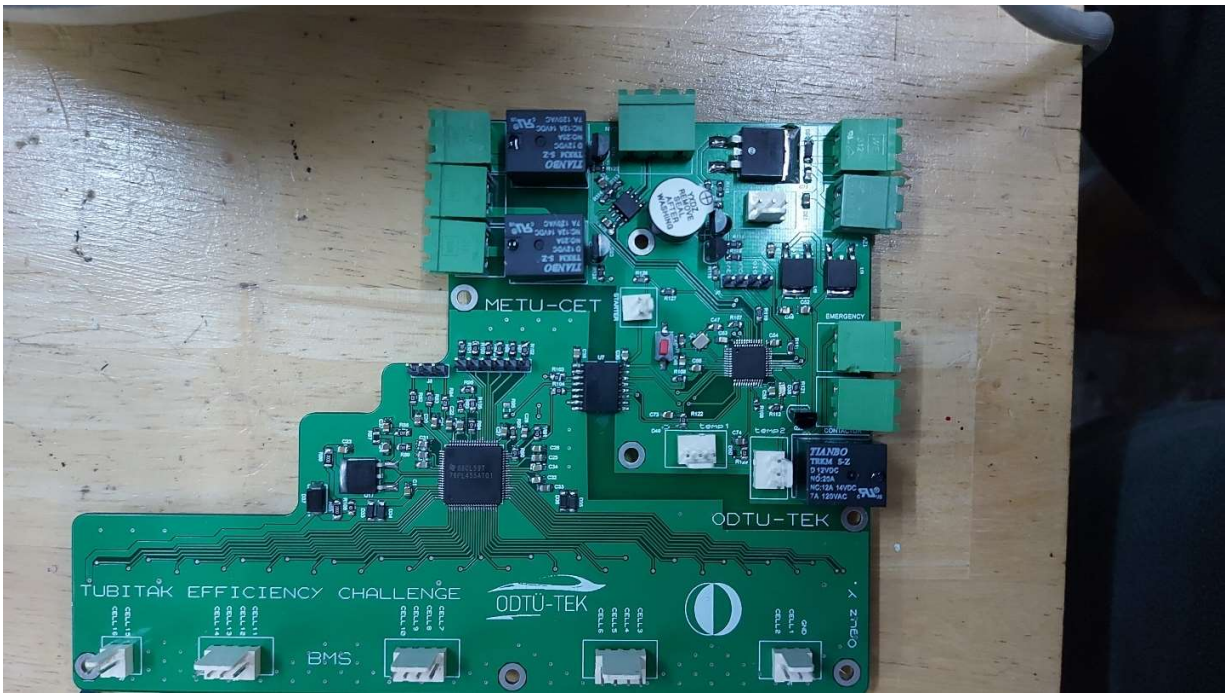

Figure 6.9: Top view of BMS

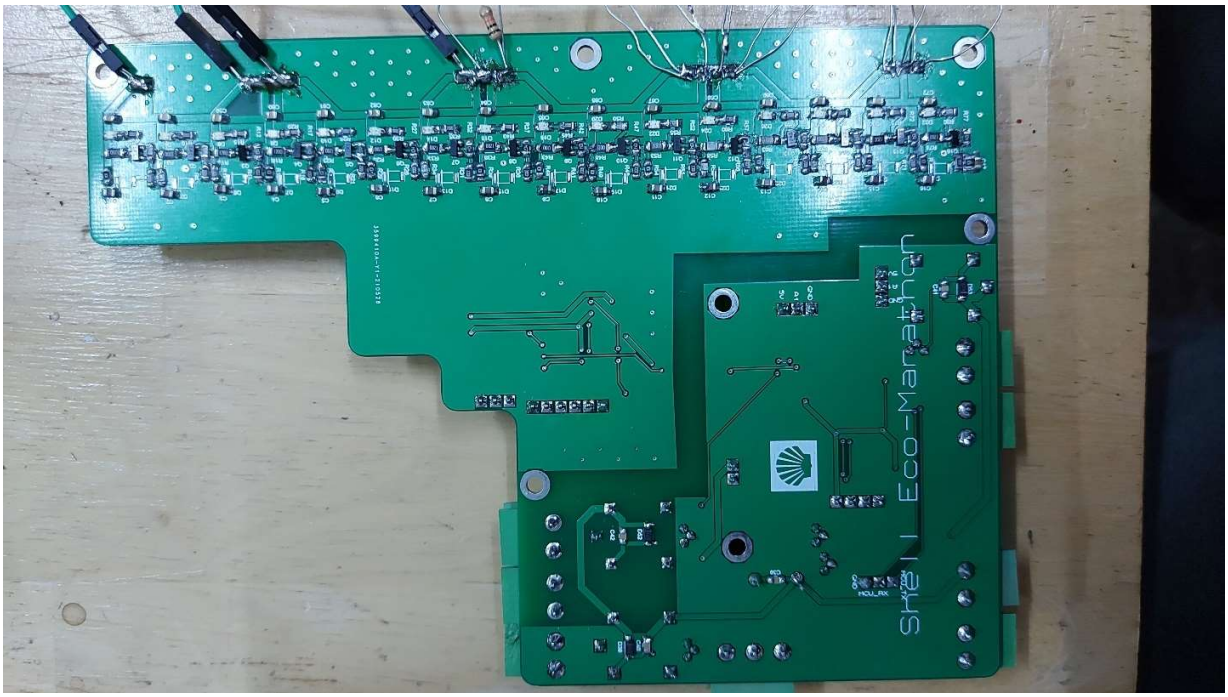

Figure 6.10: Bottom view of BMS

7. Embedded Recharging Unit

		Previous Design	New Design
Circiut Topoloji	:	Half Bridge	Half bridge
Rated Power	:	900W	900W
Output Voltage Range	:	70V	70V
Output Current Frequency	:	50 kHz	50 kHz
Input Power Factor	:	-	-
Power Conversion Efficiency	:	-	-
PWM Control IC	:	SG3525	SG3525
Protection Circiut / Components	:	Optocoupler	Optocoupler
PCB Dimensions	:	-	-

We intend to use a half bridge converter with a 50kHz frequency. The desired frequency is altered by adjusting the value of several components connected to the PWM controller, as shown in Figure 9.1. The output power of this unit will be 900W. It will be able to recharge the battery group using only one phase of the grid. Four diodes rectify the input voltage first. The MOSFETs are then controlled using a PWM controller and

MOSFET driver, and their output is fed into a transformer, which is used to scale down the primary voltage and create isolation between the input and output voltage. The power is adjusted according to the feedback signal using an optocoupler for isolation and feedback.

$$f = \frac{1}{C_T (0.7\, R_T + 3\, R_D)}$$

Figure 7.1: Formula of frequency calculation for SG3525 PWM Controller

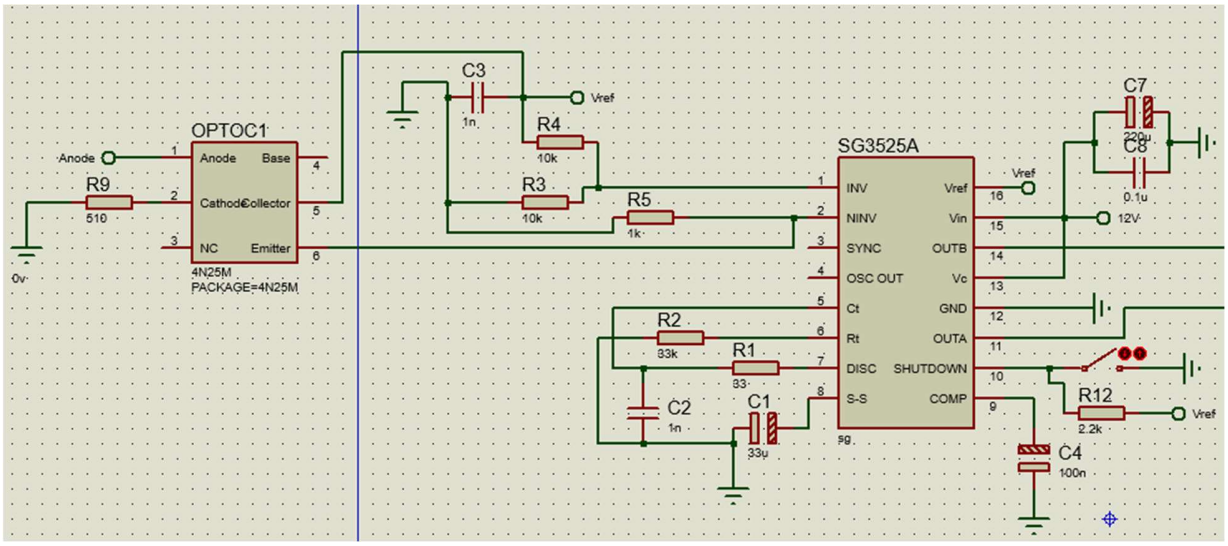

Figure 7.2: PWM Controller and feedback stage

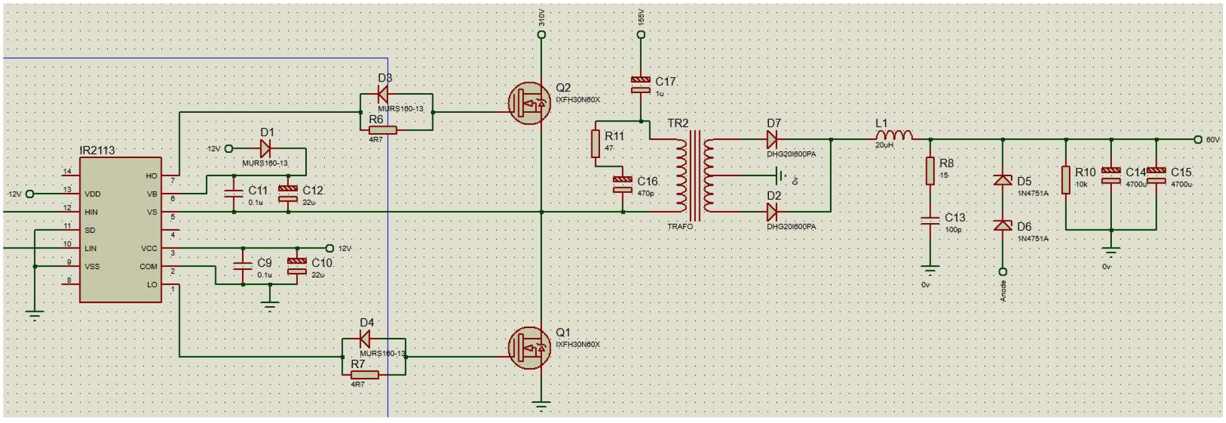

Figure 7.3: MOSFET Driver and output stage

8. Battery Packaging

At first, we were planning to use 12s10p battery, but we thought that it is not sufficient. Now, we switched to 16s12p battery since it has more capacity.

a) **Characteristics of the cells**:

We are using Sony VTC6 Li-ion batteries. It is a cylindrical(18650) type battery.

Nominal Voltage: 3.7V

Maximum voltage: 4.2V

Minimum voltage: 2.5V

Maximum charge current: 5A

Maximum discharge current: 20A

Optimum operating temperature: 23°C

Cycle Life: 500

Cell geometry: 16s12p

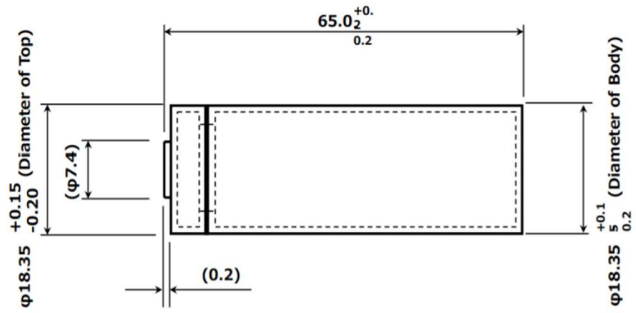

Figure 8.1: Dimensions of one battery

Figure 8.2: Sony VTC6

b) **Properties of the case materials**:

Battery, BMS, MCB, and contactor are all contained in the battery box. Because aluminum is a non-flammable material, it will be used to make the battery box. The aluminum sheet will be laser cut, wrapped all the way around the box, and then welded. Some slots will be opened to accommodate fans while also decreasing the box's weight.

c) **Thermal analysis of the battery modules/pack**:
Dimensions and airflow values were the important factors in fan selection. The results of the flow
analysis and thermal analysis of the battery box are shown in the figure below.

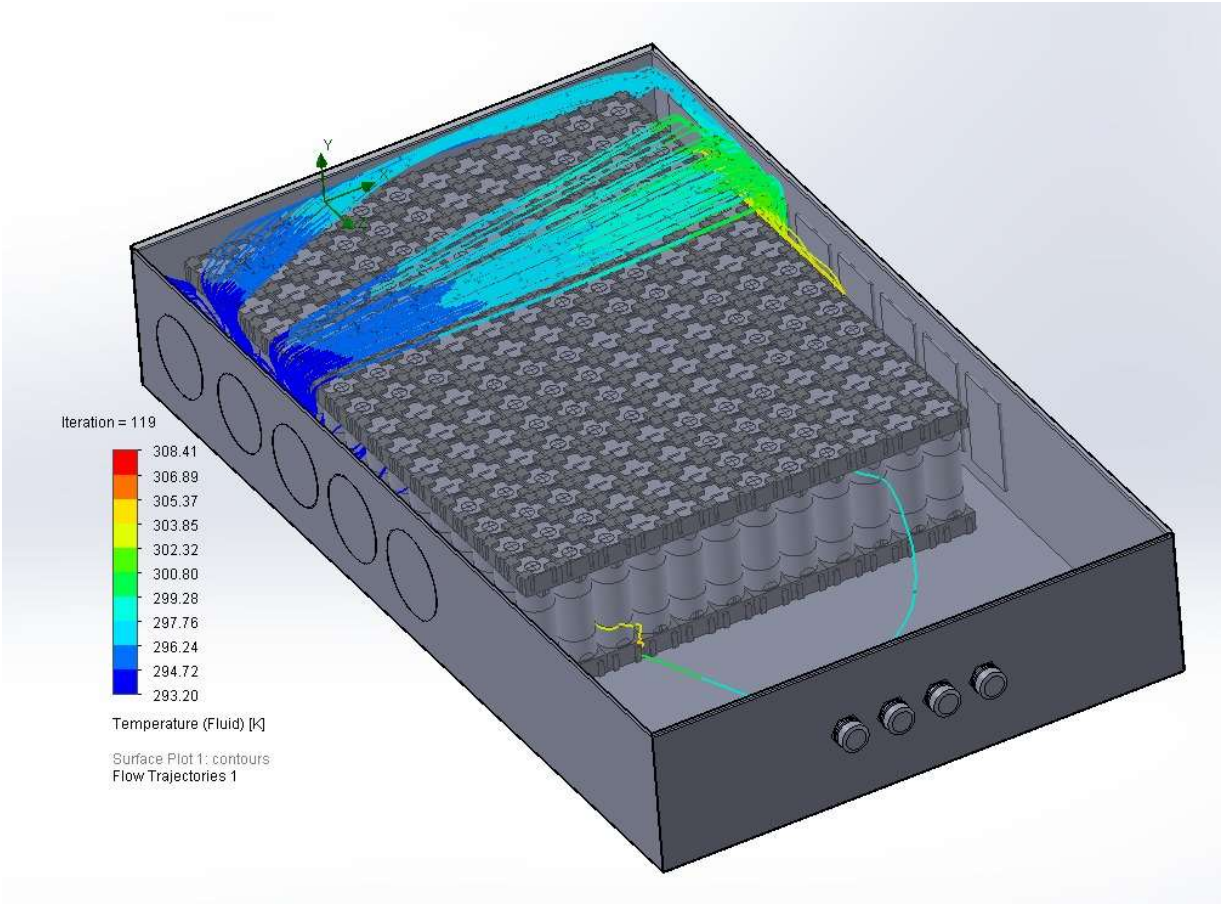

Figure 8.3: Thermal analysis of the battery box

d) **Housing and insulation of modules/pack**:

Presbant, insulating resin, thermal tape, transformer insulation paper.

e) **Battery Cooling System Details**:

On one side of the battery box, there will be four fans. The most essential considerations in fan selection were the dimensions and airflow values. The timer on the BMS will control the fans. The temperature is measured by temperature sensors, and the information is used to activate fans after a certain value is reached. Fans will work harder if the pack temperature continues to rise.

f) **Precharge circuit design (if exists):**

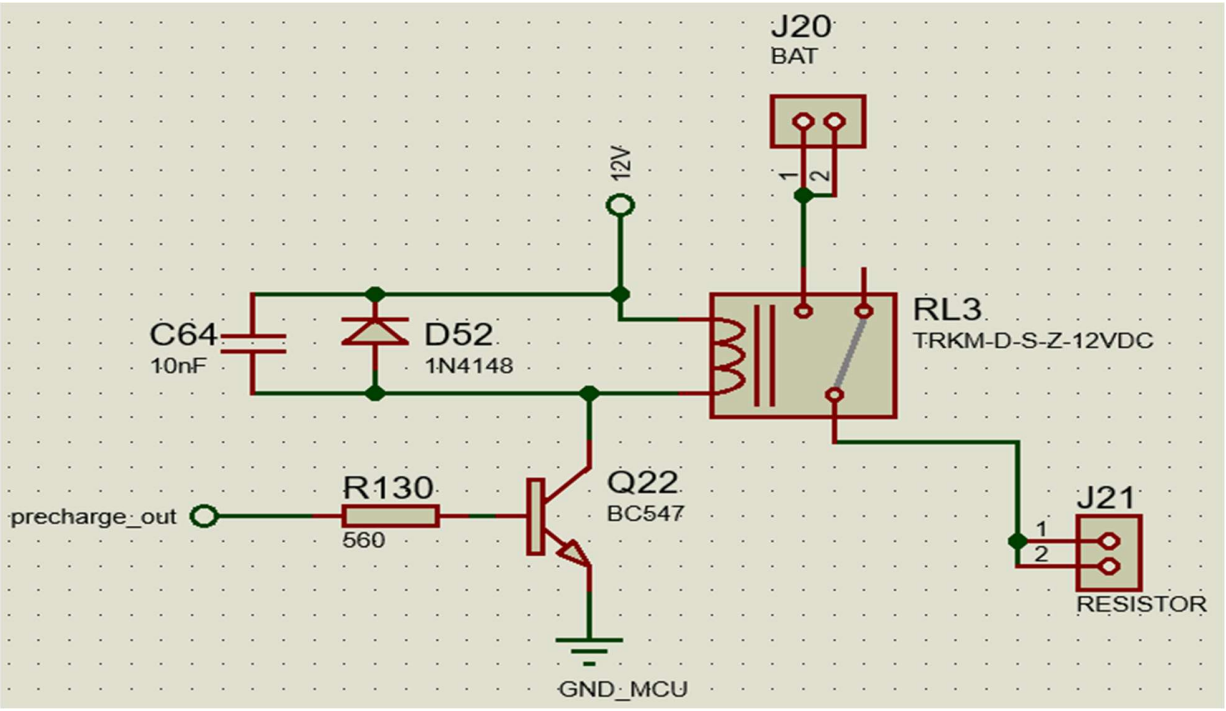

Figure 8.4: Precharge circuit

The battery's positive terminal is linked to the relay's NO terminal, and one leg of the 100 precharge resistor is connected to the relay's COM terminal. When the precharge output signal is high, the relay connects the battery to the resistor. Precharge is finished when the signal drops below a certain threshold.

9. Electronic Differential Application

Because we will only be using one hub motor to power our project, we will not be able to employ an electrical differential.

10. Vehicle Control Unit (VCU)

		Previous Design	New Design
VCU Functions	:	Warning, Data Transfer, Diagnostics	Warning, Data Transfer, Diagnostics
Controller integrated circuit	:	STM32F103	STM32F103
VCU I/O number	:	3/2	5/2
Electronic Circuit Design	:	Domestic	Domestic
PCB Design	:	Domestic	Domestic
Manufacturing of PCB	:	-	Produced in China
Software Algorithm	:	Domestic	Domestic
Experimental Study	:	Domestic	Domestic
Dimensions(PCB/Case)	:	40mm*36mm	52mm*42mm

10.1) VCU Functions

1- Monitor Vehicle’s Condition and Warning the Driver:

The VCU's screen will provide vehicle speed, battery cell temperature and voltages, motor temperature and voltage, and remaining energy data. For this, we'll use a Nextion HMI screen. The VCU and the screen interact through UART.

2- Signal Acquisition and Data Transfer:

The transmitter on the automobile will provide vehicle speed, battery cell temperature and voltages, motor temperature and voltage, and remaining energy data to the receiver in the monitoring center through RF modules. We intend to use the HC-12 wireless communication module, which communicates through UART and has a range of 1km.

3- Diagnostics:

We design a GUI in Nextion Editor which is a specific program for Nextion screens. If there is an overvoltage or undervoltage of cell voltages, it gives a warning in the screen and informs the driver. If there is any circuit unconnected from the system it will create a warning, too.

10.2) Electronic Circuit Design

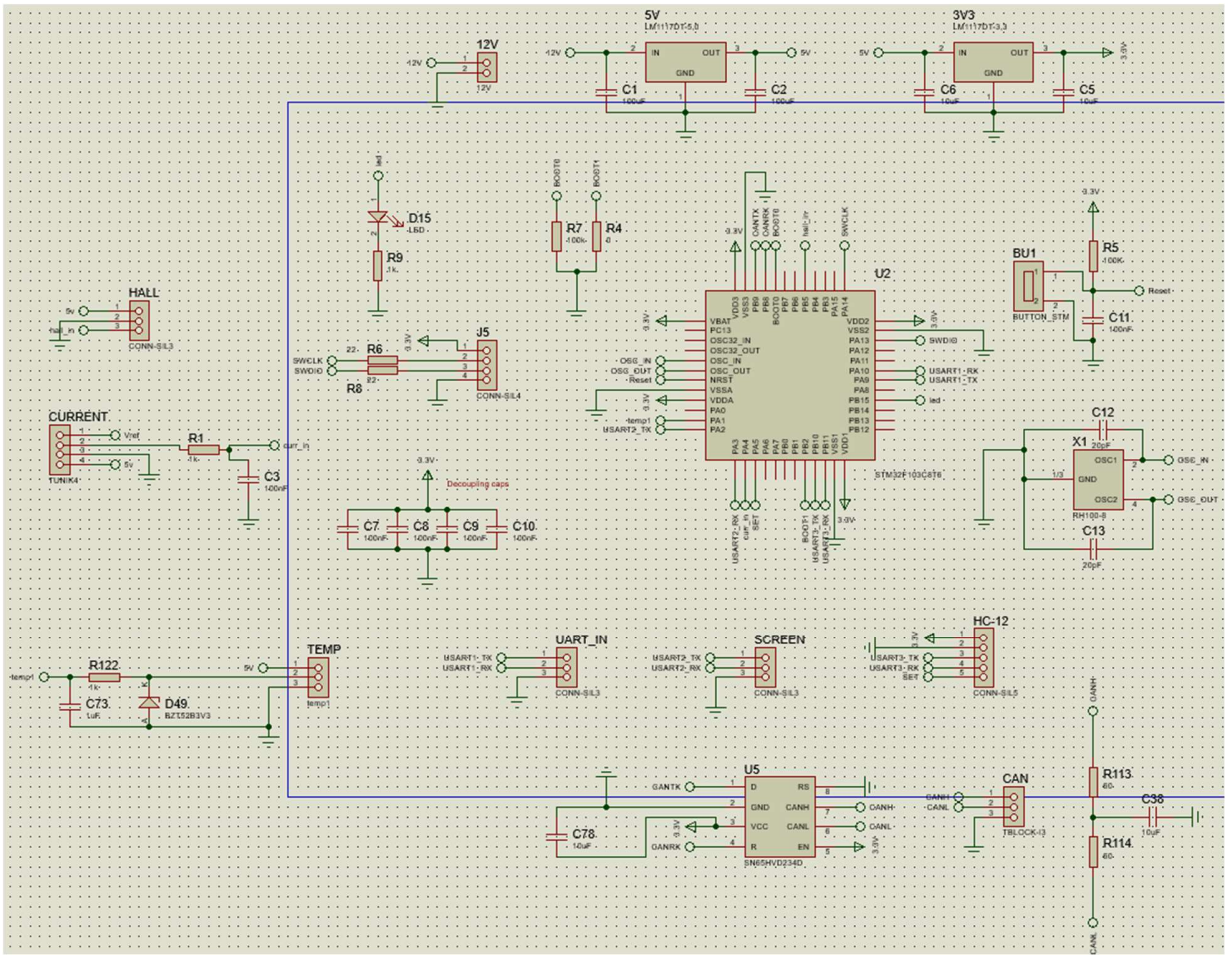

Figure 10.1. VCU circuit

10.3) Printed Circuit Design

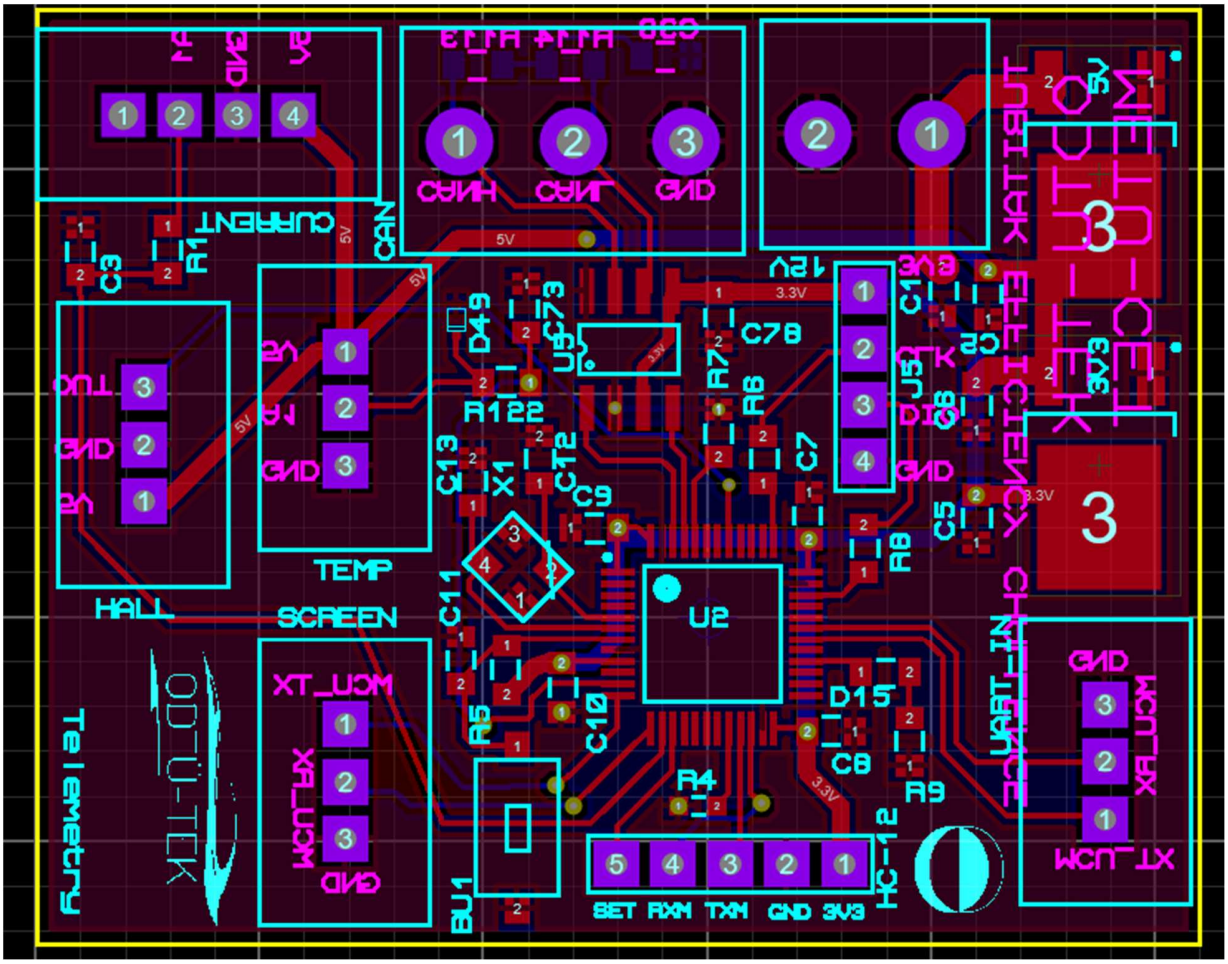

Figure 10.2: VCU circuit (Telemetry Transmitter)

We use the STM32F103 as the MCU in the VCU, and we use blue pill which uses the same chip as MCU for the telemetry receiver. We did not produce a PCB for the receiver since it's a very small circuit and has one job. We use CANBUS and UART to get the data. We communicate through UART to send data to both the screen and the telemetry receiver.

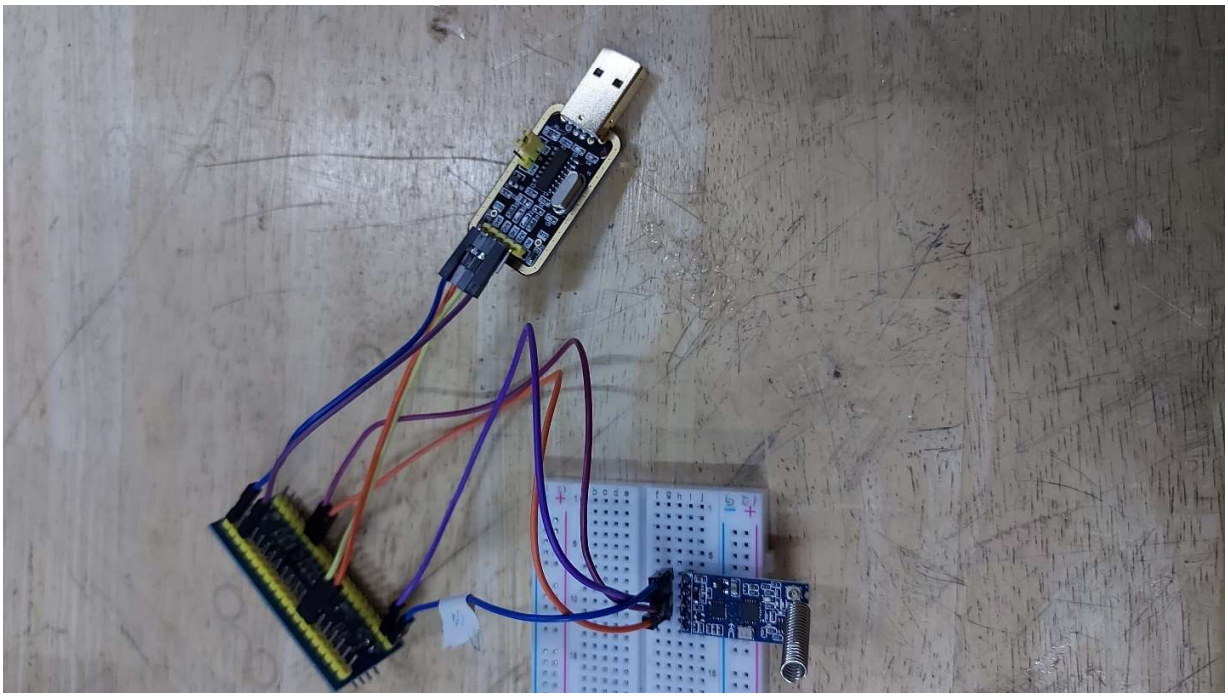

Figure 10.3: Telemetry Receiver

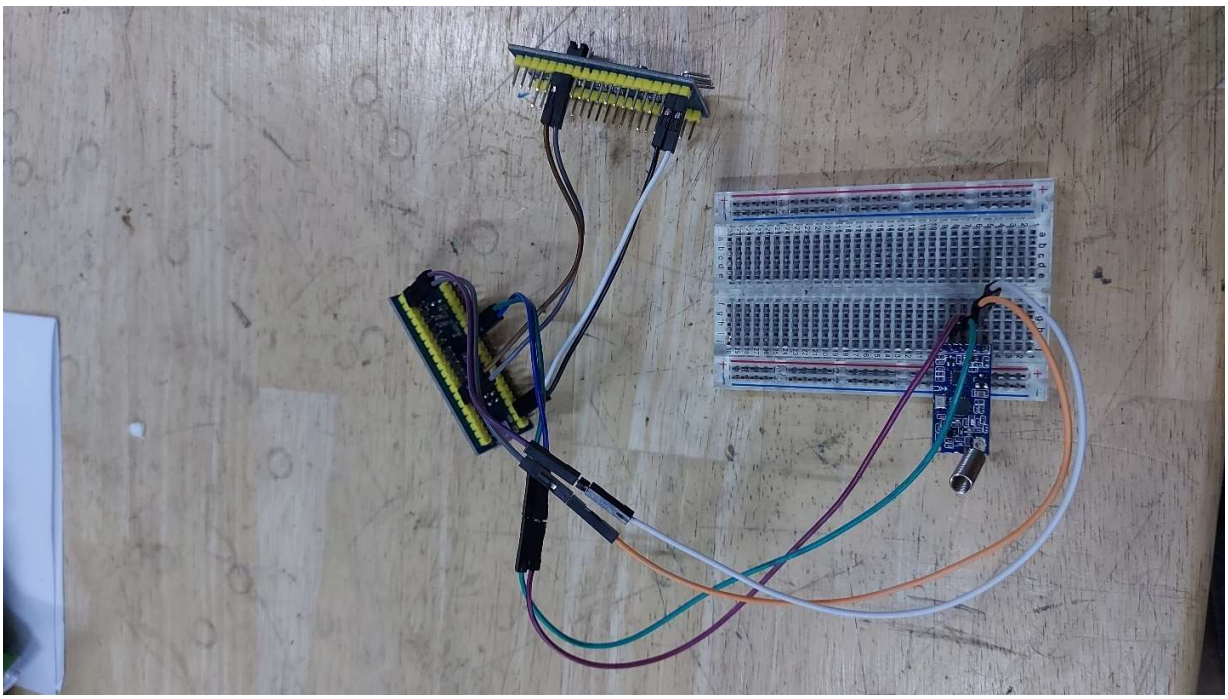

Figure 10.4: Telemetry Transmitter for test representing the PCB

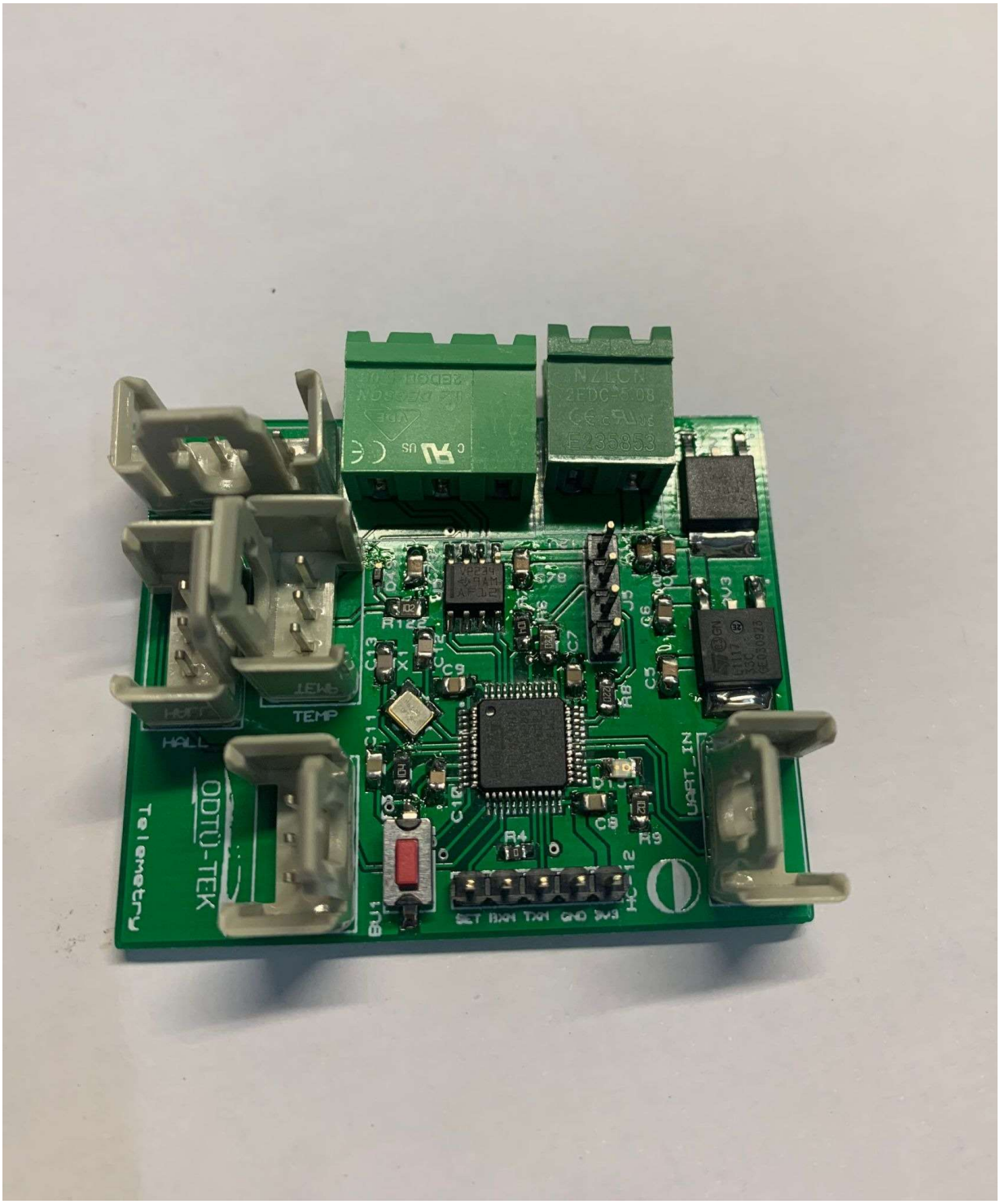

Figure 10.5: Telemetry Transmitter(VCU)

While we are waiting for the delivery of the PCB of the telemetry, we tested the Telemetry Transmitter representing the system with PCB. In Figure 10.4, bottom blue pill represents the VCU, upper blue pill represents the screen. In telemetry receiver, a blue pill receives data from HC-12 and transmits that data to PC via USB to TTL. Finally, by processing that data in Python, necessary data is shown at an interface. After the delivery of PCB, we tested it and it works fine.

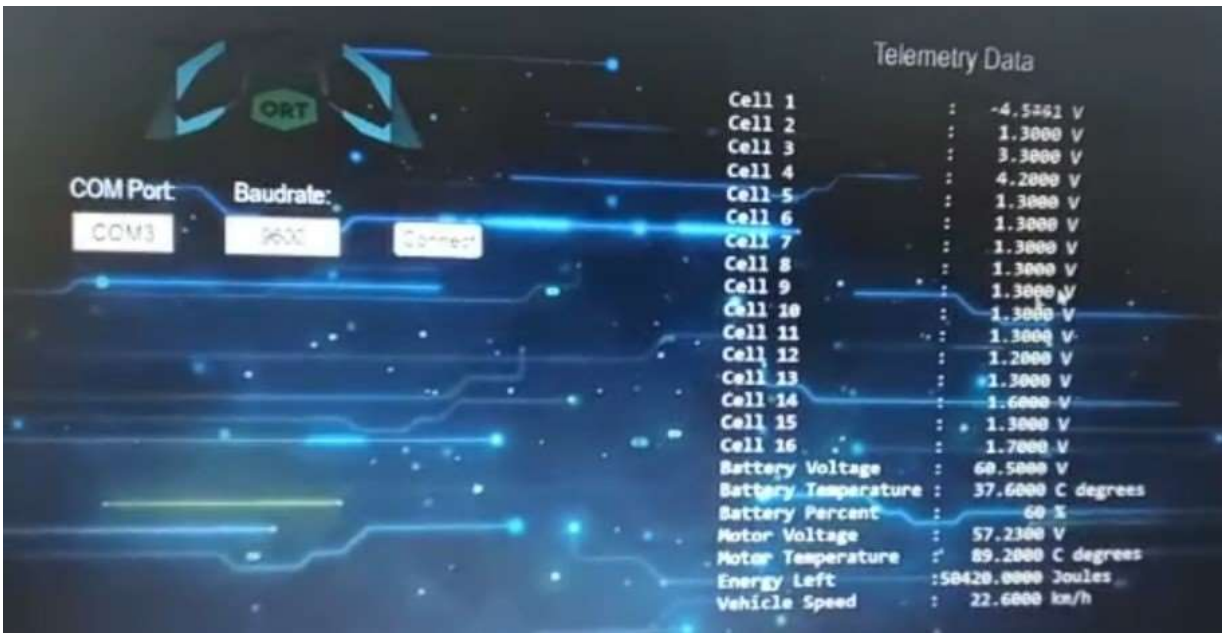

Figure 10.6: Telemetry Interface

11. Isolation Monitoring Device

		Previous Design	New Design
Integrated Microcontroller	:	-	Arduino nano
Measurement method	:	-	Analog
Modeling Period	:	-	50 ms
Measurement Precision for 100kΩ	:	-	+-624Ω
Measurement Precision for 1MΩ	:	-	+-4.88k Ω
Dimensions(PCB/Case)	:	-	50mm*100mm*30mm

a) Circuit Design

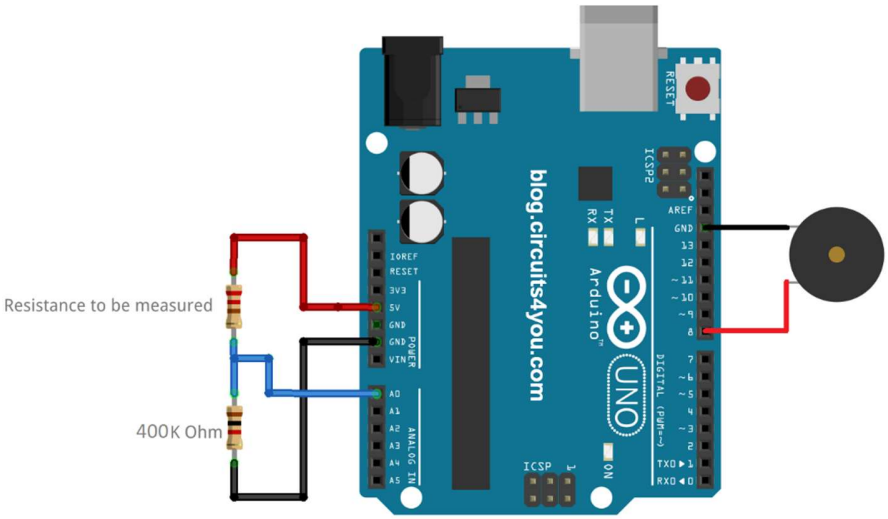

Figure 11.1

b) Simulations

We made some simulations using online sources (https://www.falstad.com/circuit/circuitjs.html) and our results were successful

c) Currently we have not worked on printed circuit board for our circuit

d) We made a small prototype using breadboard and jumper cables.

e) We tried the prototype circuit on our chasis and our circuit successfully measured and reacted to the change in resistance.

12. Steering System

12.1 Design

Designing a proper suspension and steering system is essential for a vehicle that is built for efficiency. An improper steering and suspension system can create both safety issues and energy losses. We designed our suspension and steering system with those in our minds.

The first design decision we made was to decide the type of suspension system. Considering safety, minimum energy losses, ease of manufacturability, and manufacturing costs, we decided to implement a double-wishbone suspension in both front and rear.

At the initial stage, we used vsusp.com for designing the system in two dimensions. Those are our design criteria for suspension kinematics:

- Minimizing scrub radius for reducing the forces on the steering system
    - It is less than 1 mm
- Minimizing the forces on bearings for increasing the lifetime and efficiency of bearings
- Optimizing the position of the roll centers with respect to the center of mass for a stable drive
    - Front and rear roll centers are 100 mm and 107 mm away from the ground, respectively.
- Minimizing the movement of the roll centers for a predictable drive
    - Less than 10 cm in the case of 5° roll for both front and rear
- Giving a small amount of negative camber to increase cornering performance
    - -0.2°
- Minimizing the camber gain during bump and rebound
    - Less than 2° in 30 mm bump
- Minimizing the camber gain during roll
    - Less than 3° in 5° roll

Our final 2D design can be seen in figures 1 and 2.

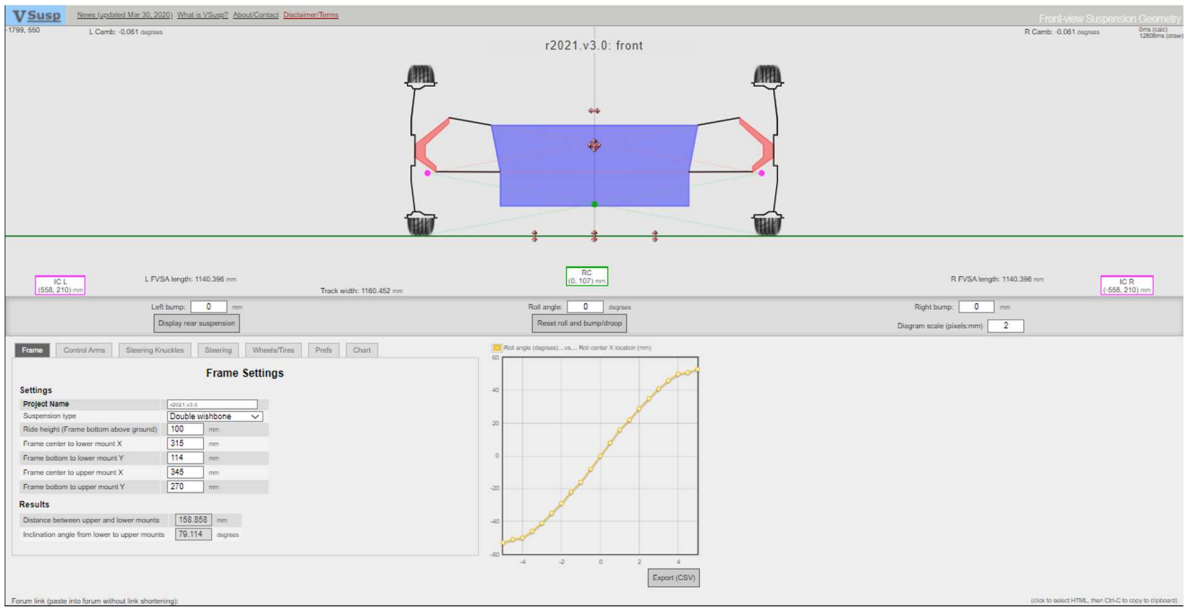

Figure 1: 2D design of our front suspension

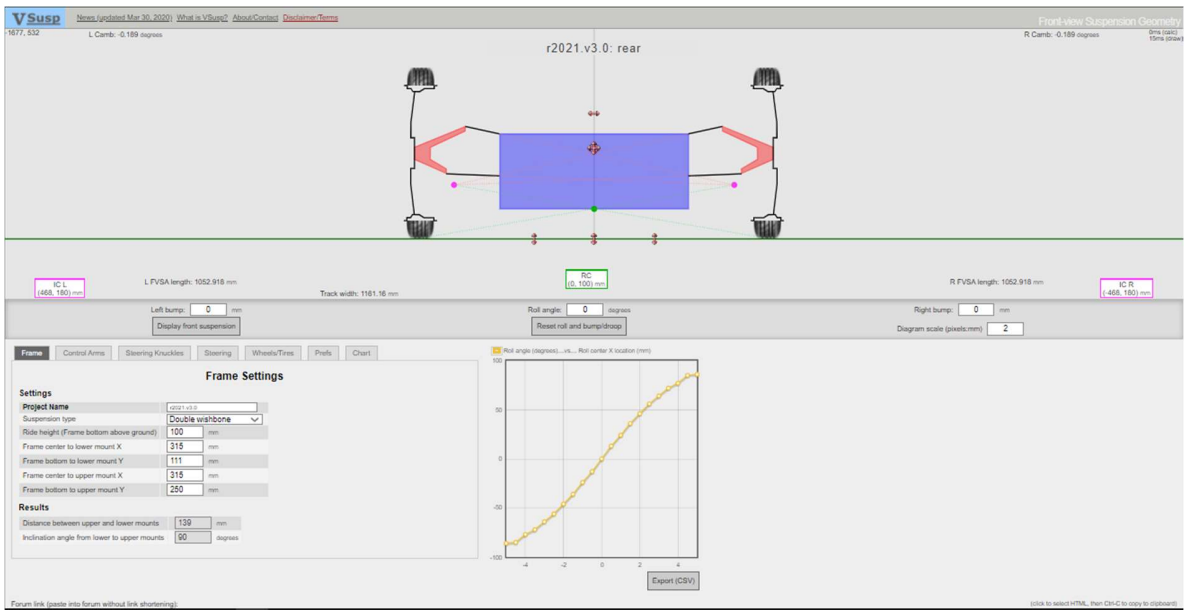

Figure 2: 2D design of our rear suspension

After designing the 2D suspension kinematics and deciding the wheelbase (2000 mm), we started to design our steering kinematic in two dimensions. To do that, we wrote a script in MATLAB using Hanzaki, Rao, and Saha's (2007) method to optimize the knuckle, tie rod, and steering rack dimensions. After the 2D design, we combined suspension and steering kinematics to obtain a complete car model. We continued kinematic analyses in Lotus Suspension Analysis v4.03 program using the entire suspension model of our car. We considered the following criteria while designing the steering kinematic and finalizing the 3D suspension kinematic design:

- Minimizing the slip angle in both slow and fast cornering (That decreases the rolling resistance, thus increases the efficiency)
- Optimizing the Ackermann percentage
    - Between 123% and 86% while cornering
- Minimizing the steering error
    - The maximum steering error is 0,47°
- Optimizing the steering ratio
    - Approximately 7:1
- Ensuring enough minimum turning radius for maneuverability
    - 3,41 m according to the bicycle model
    - 4,40 m according to the SAE outer wheel center
- Minimizing the bump steer for safety
    - Less than 1,3° for both front and rear
- Giving enough amount caster to ensure responsive steering experience (It also causes the steering wheel to return its forward position by itself)
    - Approximately 1,6°

Our 3D suspension kinematic design and some valuable graphs in Lotus Suspension Analysis program can be seen in figures 3, 4, and 5.

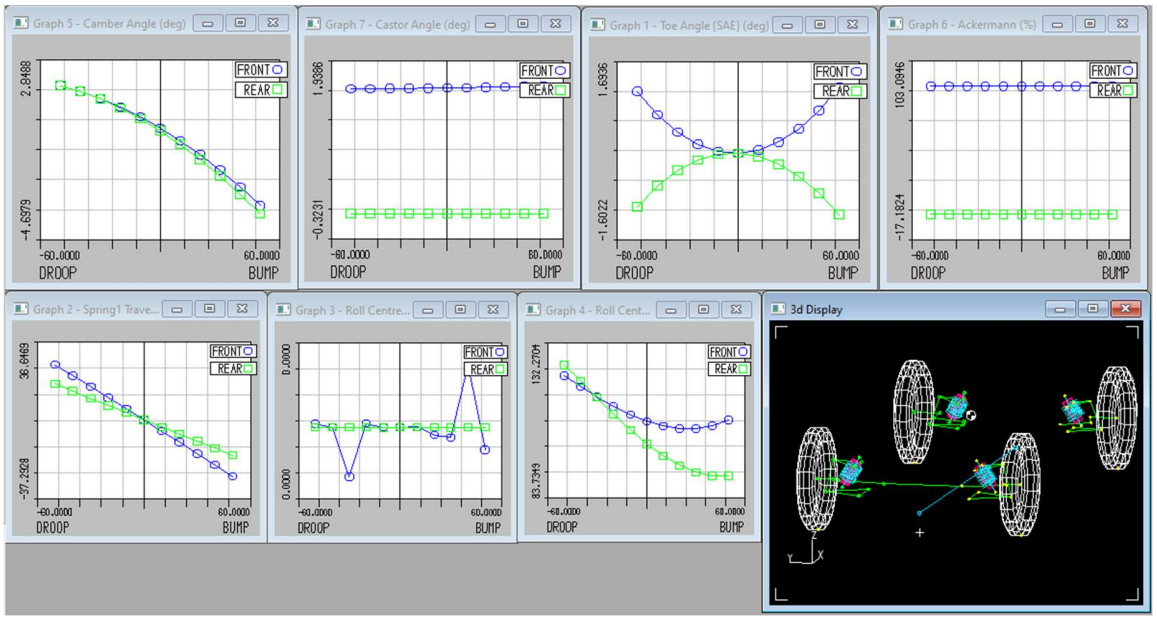

Figure 3: the behavior of our suspension and steering system in bumps

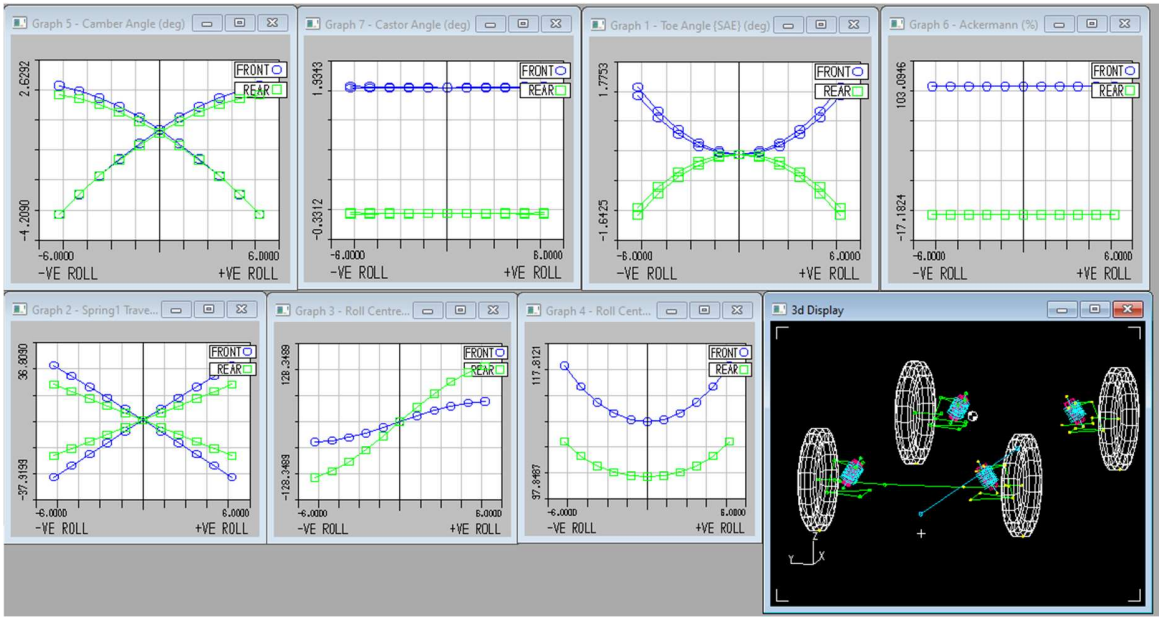

Figure 4: the behavior of our suspension and steering system in roll

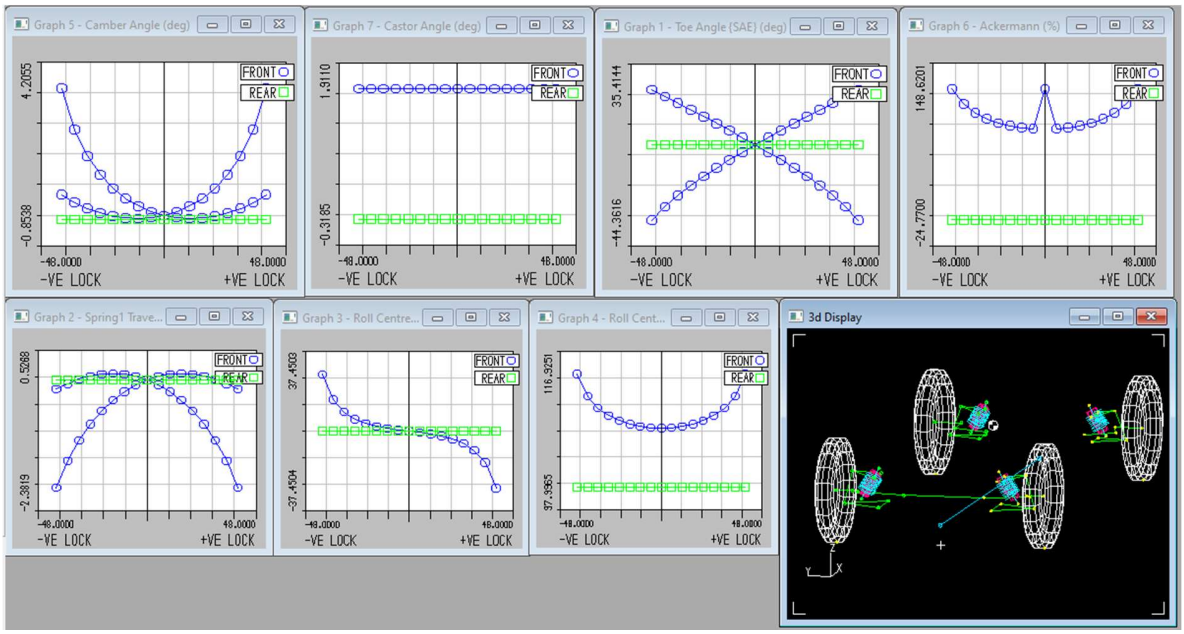

Figure 5: the behavior of our suspension and steering system while steering

The relation between inner and outer wheel turning angles can be seen in figure 6. In that graph, you can see both Ackermann steering (ideal steering) and our design (theoretical calculation according to our 2D kinematic design). The difference between these two is defined as steering error. You can also see that the maximum steering error is 0,47°. That means our design is nearly identical to Ackermann steering. This way, we can eliminate the tire slipping at slow speeds. Reducing slip angle reduces the rolling resistance of the tires significantly. Thus, efficiency is increasing.

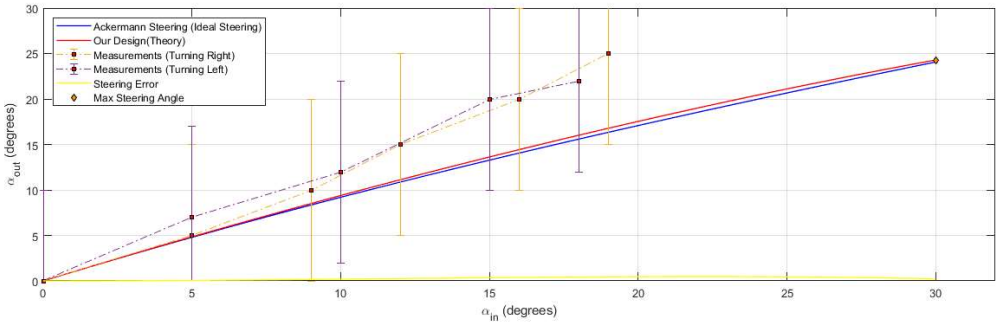

Figure 6: The relation between inner and outer wheel turning angles

In figure 7, you can see the relation between the steering wheel turning angle and inner and outer wheel turning angles. As seen on the graph, the maximum angle that the steering wheel can turn is 220° on one side. The system is symmetric on both sides. Because of that, the total angle that the steering wheel can turn is 440°. However in our design such movement is not necessary. Because of that we limited the movement pf the steering rack such that steering wheel can rotate 150° on one side and 300° for total.

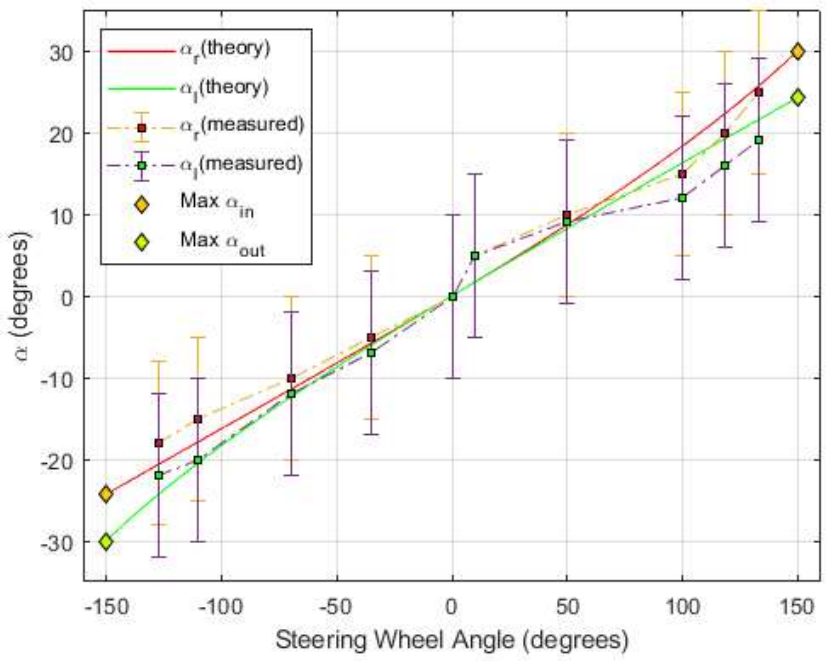

Figure 7: The relation between steering wheel angle and wheel turning angles

In figure 8, you can see the relation between steering wheel turning angle and turning radius calculated for both the bicycle model and SAE outer wheel center. When the steering wheel turns 220°(maximum), the turning radius according to the bicycle and SAE outer wheel center models are 3,41 m and 4,40 m, respectively.

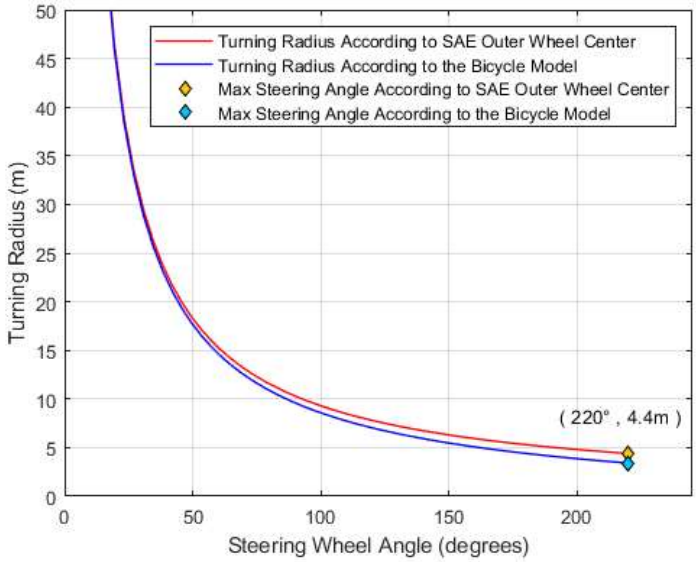

Figure 8: The relation between steering wheel angle and turning radius

After designing everything kinematically, we designed the actual 3D parts in suspension and steering systems. We calculated the forces in very different scenarios and decide a part is suitable for that job or not by calculating the stresses on the parts. Our design goal is to ensure that every part is as lightweight as possible while maintaining the factor of safety(in the most extreme load scenario) larger than 1,5. We used Solidworks Simulation and Ansys Mechanical for calculating stresses and factor of safety (FOS) values. By using the results of those structural analyses, we decided on the materials that we use. Most parts will be made out of Al 6061-T6 alloy. However, in some parts, we will use some steel alloys like AISI4140 and AISI4340.

You can see the drawings of front suspension and steering systems in figures 9 to 12.

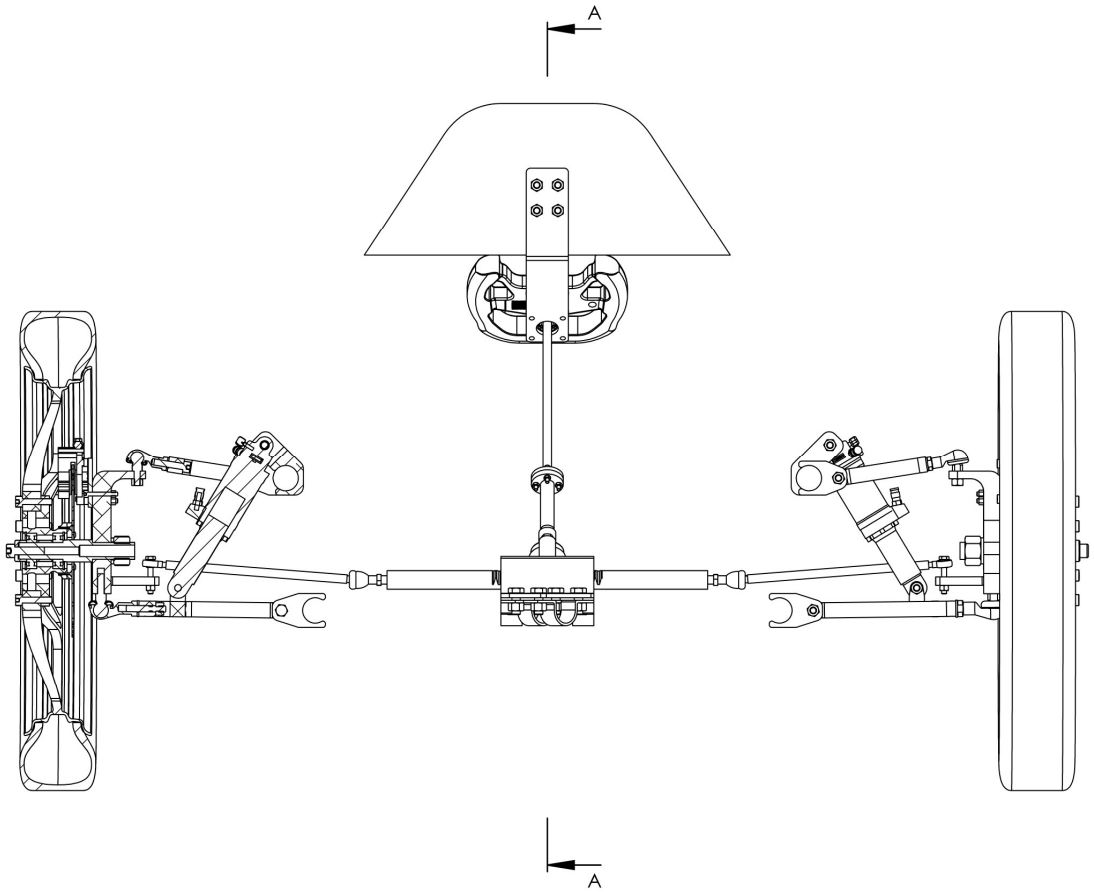

Figure 9: Front suspension and steering system from front

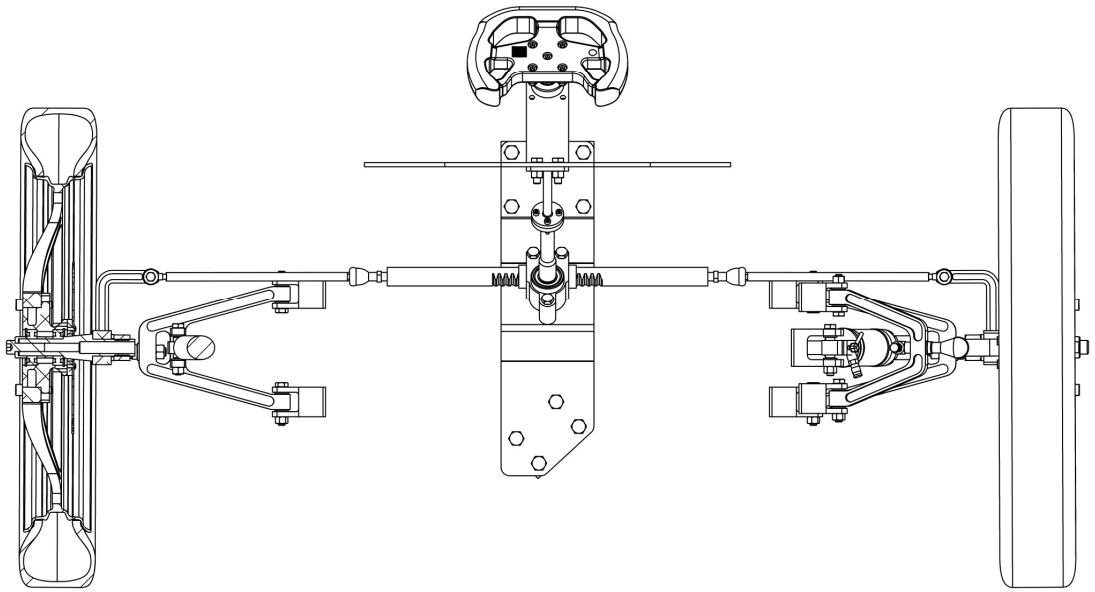

Figure 10: Front suspension and steering system from top

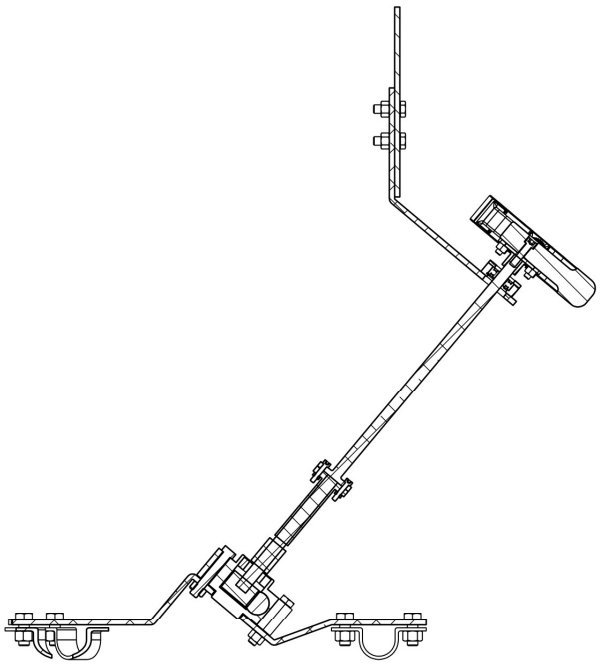

Figure 11: Steering wheel assembly from right

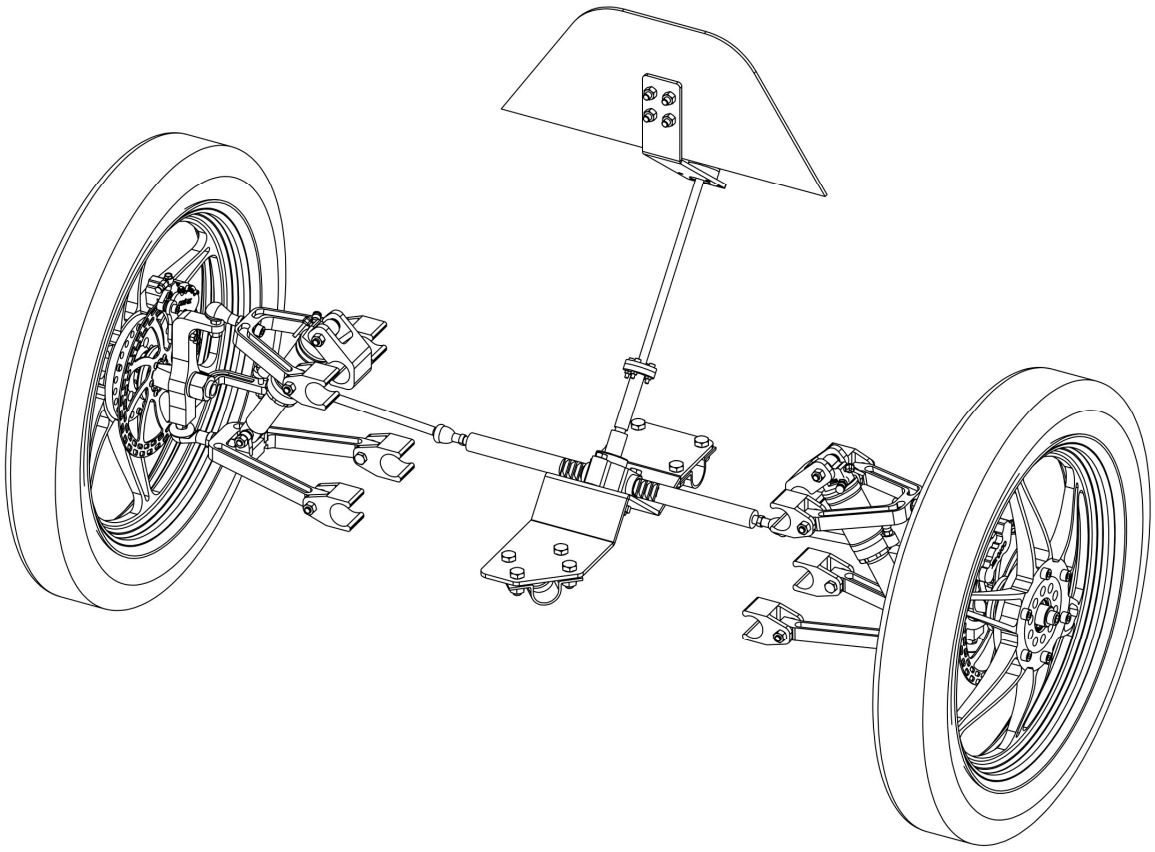

Figure 12: Front suspension and steering system trimetric view

You can see the drawings of rear suspension system in figures 12 to 14.

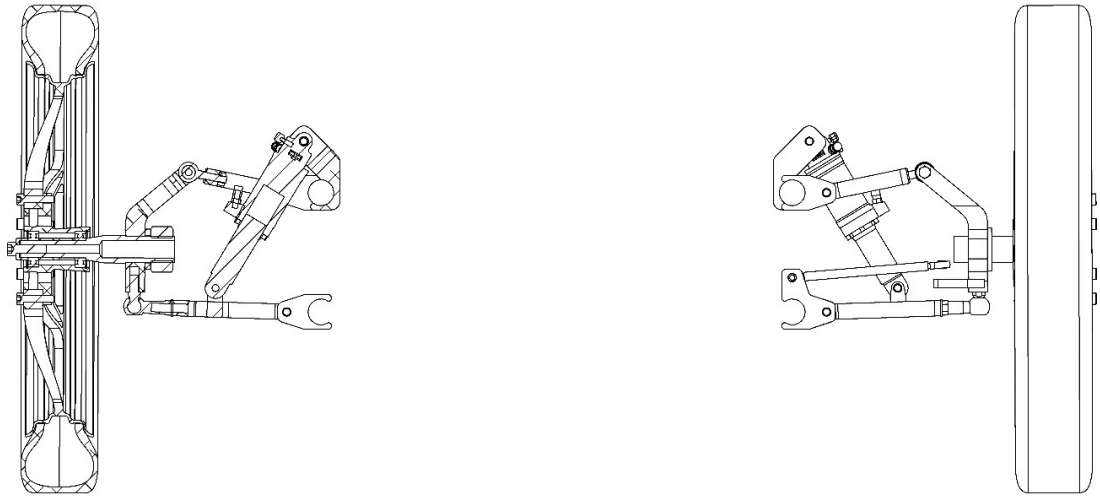

Figure 13: Rear suspension system from front

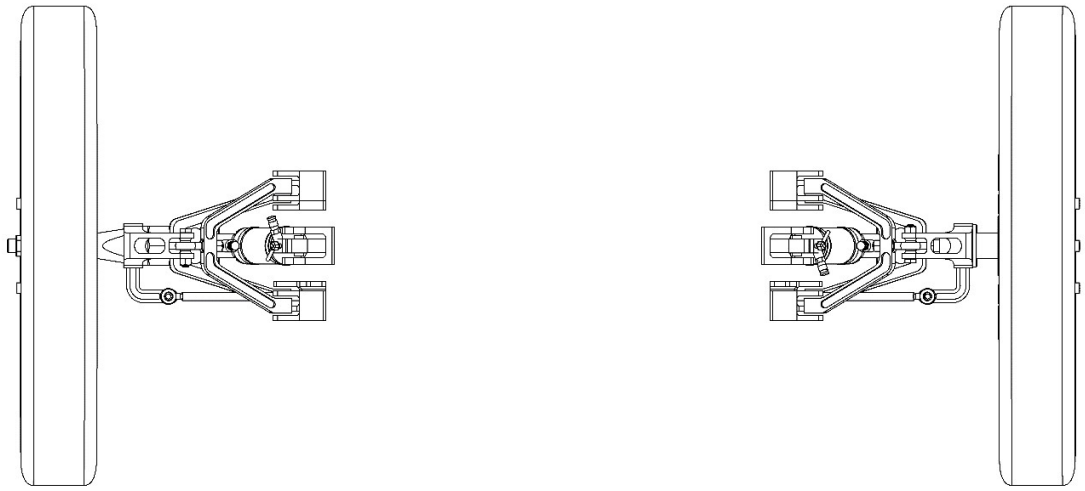

Figure 14: Rear suspension system from top

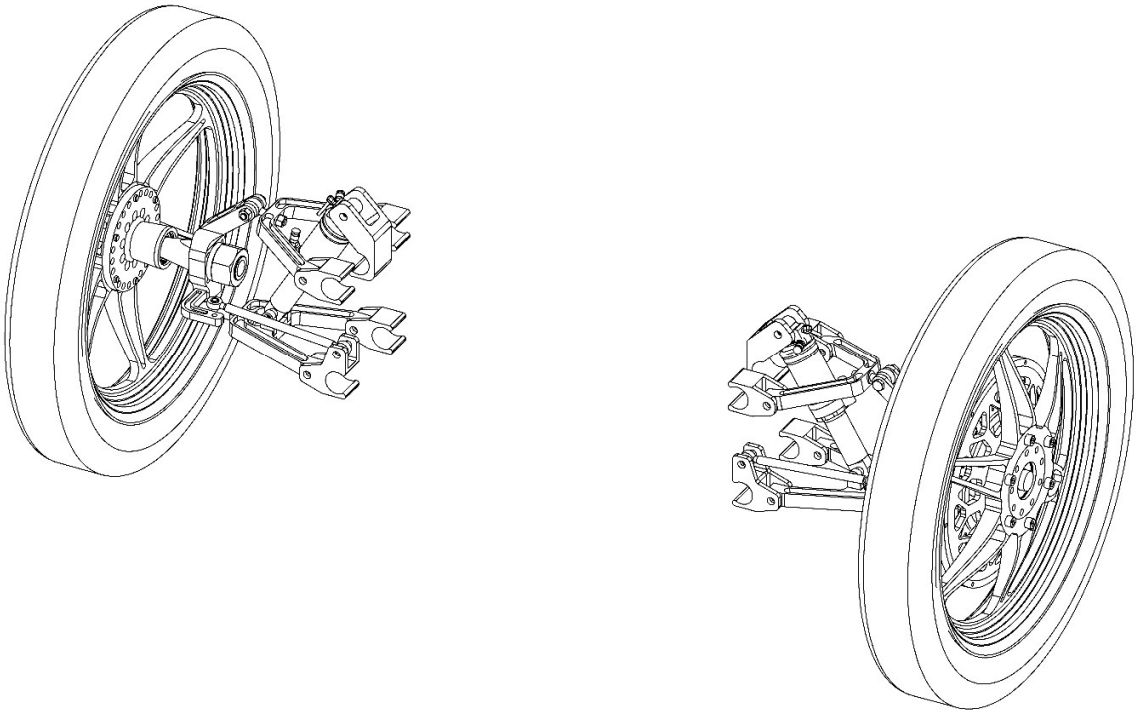

Figure 15: Rear suspension system trimetric view

You can find the 3D model of the front suspension and steering system and some additional files in the following Google Drive folder:

https://drive.google.com/drive/folders/10fi9Klkx_jUY8kKhoEh3vz4Sewx--5lC?usp=sharing

12.2 Production

The first thing we did for producing steering system is to decide which parts we will buy ready and which parts we will design and produce from start. Since we had a steering rack and pinion gearbox in hand from previous years, we decided to use them to save money. The other thing we used as ready is ball joints and bearings. Other than those we produced every part from zero. We used milling, turning, laser cutting, bending while producing the indivifual parts. For assemble them, we used welding some of the places and fasteners for the rest.. You can see the final assembly of the steering system in the following figure.

Figure 16: Final assmebly of the steering system

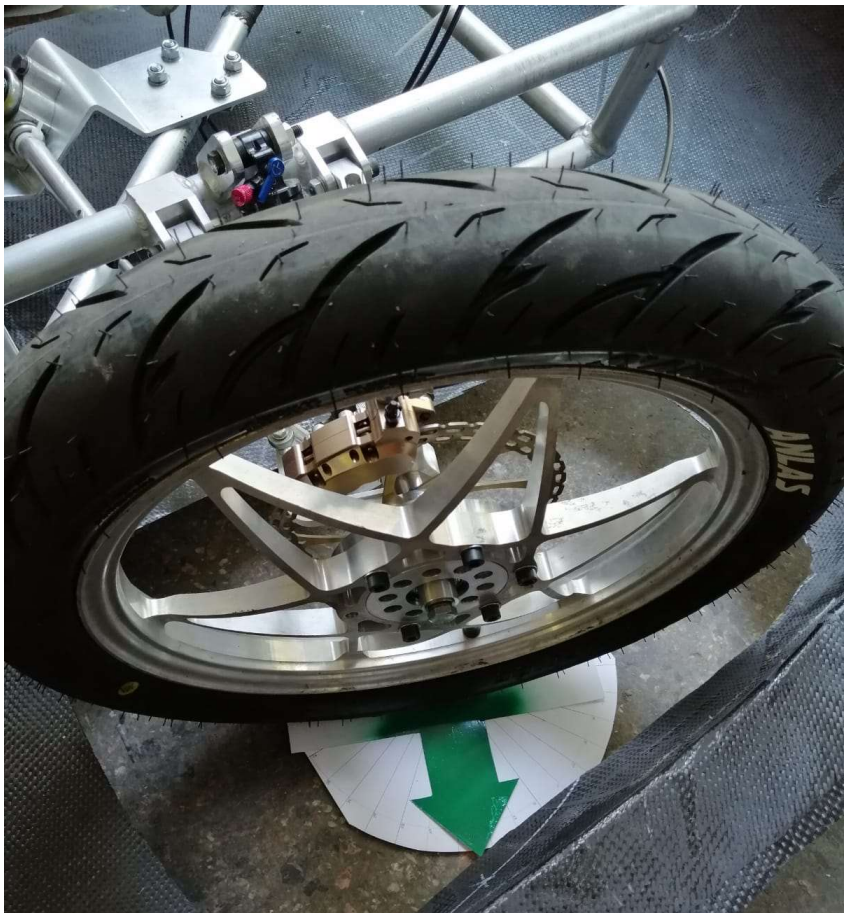

Figure 17: Steering angle measurement process

References

Papaioannou, G., Gauci, C., Velenis, E., & Koulocheris, D. (2019, August). Sensitivity Analysis of Vehicle Handling and Ride Comfort with Respect to Roll Centers Height. In The IAVSD International Symposium on Dynamics of Vehicles on Roads and Tracks (pp. 1730-1739). Springer, Cham.

13. Door Mechanism

In terms of locking mechanism, we decided to further develop the previous mechanism, which is consisted of a spring-loaded latch bolt and a 3d-printed lever handle. We decided to keep the latch bolt mechanism as it was simple and reliable. However, as the regulations have changed and there was still room for improvements, it was a necessity for us to add new things on top of the old design. First, as the regulations demanded a new locking mechanism that can be only opened by key –not by force or turning the lever handle- we decided to cut the middle part of the latch bolt and place a totally independent deadbolt. We used a peg-and-slot mechanism in order to provide linear motion for the deadbolt. We also placed the key slot on the same circular part (crank) that has the peg on it. This way, when the key slot turns with the key, the whole crank turns –including the peg-, thus the deadbolt moves forward. We also decided to design a new lever handle that won't disturb the air much. In the previous design, the lever handle was sticking out of the shell which causes energy loss in form of aerodynamic drag. To prevent this, we contrived a new door handle that is similar to what you can find in Tesla Model 3 or TOGG. This new design doesn't stick out and causes drag until you push it. With these changes, we achieved to minimize drag caused by door handle and redesign our previous lock according to new rules.

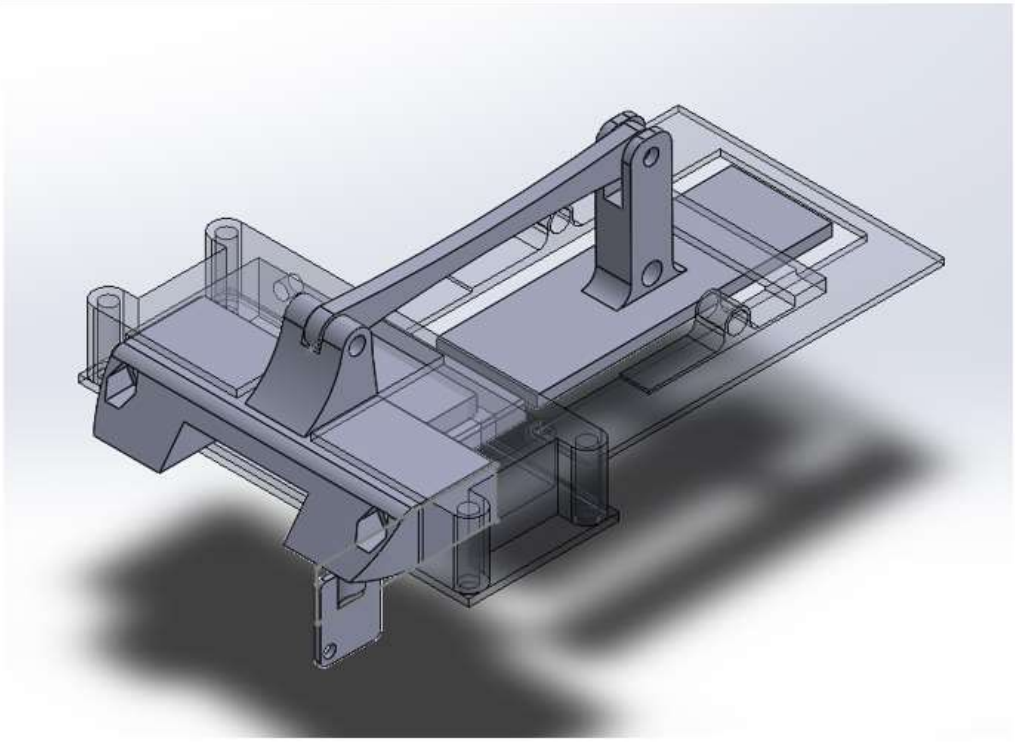

Door locking mechanism

PS: The distance between the handle and the bolts are shortened in the figure above for convenience

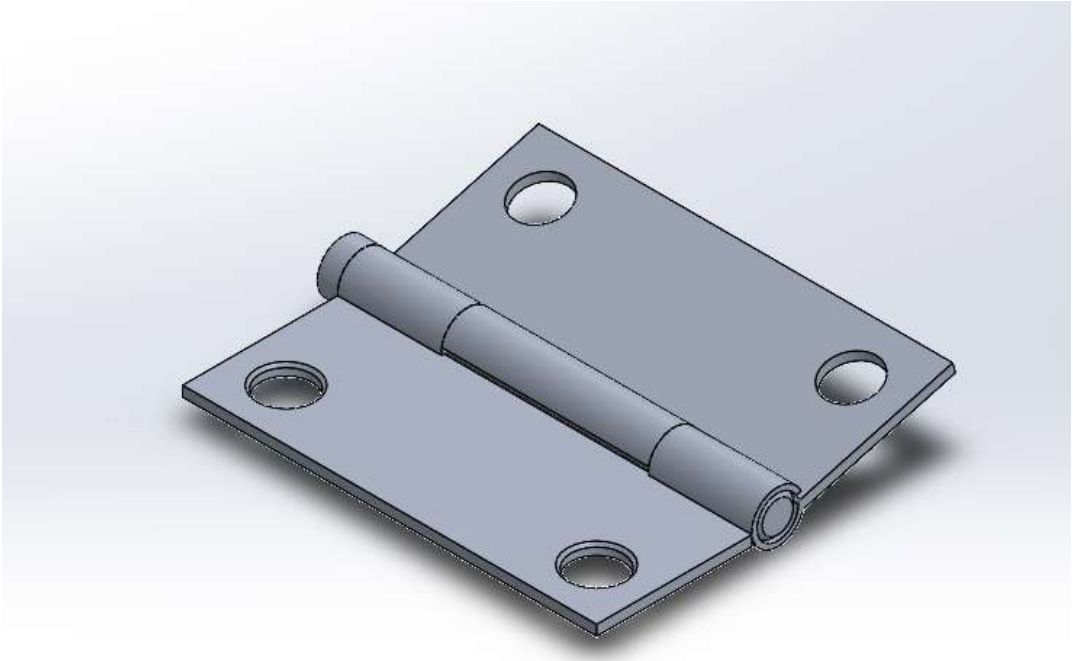

Door Hinge

We placed the door hinge on the lower part of the door where it becomes almost flat.. The curved surface of the door left us with limited options for us to choose where to place hinges. As the surfaces of the hinges shoul be parallel to each other, we chose the most flat part of the door and assembled both hinges close to each other as possible to suffer less from the negative effects of curvature. We found the optimal location with a series of equations. The doors are nearly 2,5 kilograms and the center of mass is located 270 mm above the bottom of the door. The hole that carries the hinge on the lowest part of the door is only 6 mm high from the bottom of the door. Let the h_1 be the height of the centre of mass of the door, m is the mass of the door and g is the gravitational acceleration;

$$m \times g \times h_1 = 2,5 \times 9,8 \times 0,27 = 6,615\ Nm$$

We know that we need a moment that has a magnitude of 6,615 Nm. It is hinges' duty to provide this moment and keep the static position of the door. This means that if we want to provide this moment of 6,615 as easy as possible, we should place the hinges as high as possible. This left us with two opposite demands. The logic of how hinges work demands us to place the hinges low as possible so they will be less effected by the

curvature. Yet, the moment we should provide can be generated much more easily by placing them higher. This led us to find a specific region where the curvature changes too much so that we can place hinges just before that region. If you can imagine the curvature of the door as a mathematical function, you can think the property mentioned here as the derivation of this function, or the instant incline. The point where the derivation of this function is higher means that the curvature is changing more rapid than every other point. We tried to place the hinges right before this point where the derivation of the function at that point is the highest.

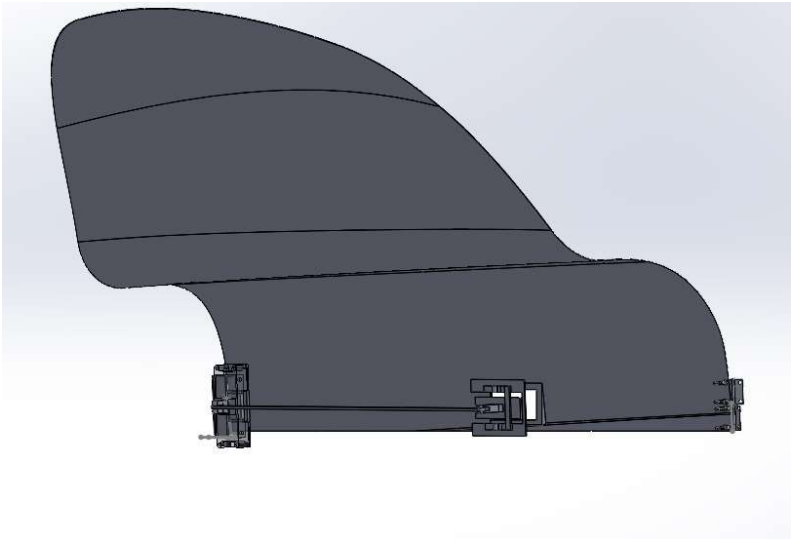

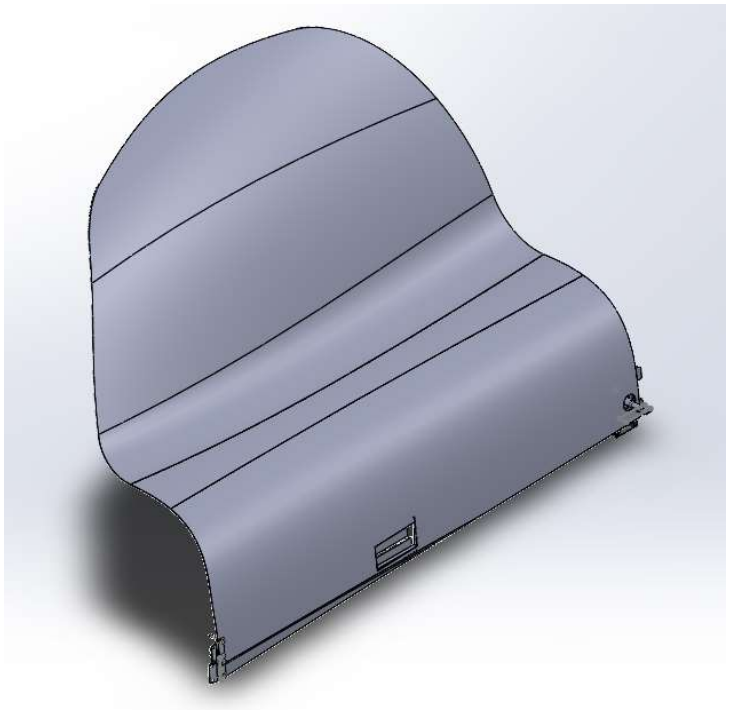

There are two symmetrical doors on the vehicle, on both sides which provides ease to the both the driver and the passenger when they want to get out. According to the measurements we made on Solidworks, the surface area of each door is approximately 0.95 m^2.

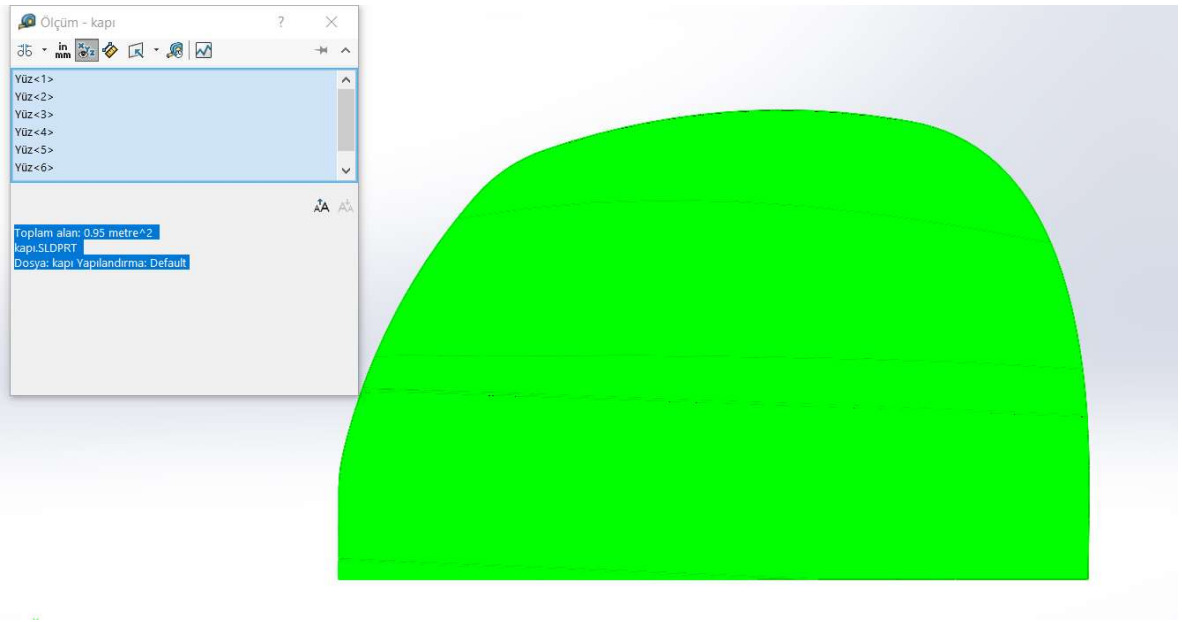

To guarantee, that no 0,2 mm thick object can enter from the door when its closed, we cut the door with a grinding machine that has a cutting kerf smaller than 0,2 mm. Moreover, for the unexpected gaps occurred during the production, we used door seal. Finally, with the help of angled deadbolt and latch bolt in our locking mechanism, it is possible to close the door just by pushing and not needing to use the door handle. When the door is locked, door handle is no use without the key as the deadbolt mechanism is totally independent from the mechanism related to handle.

14. Mechanical Details

A. Technical Drawing of the vehicle

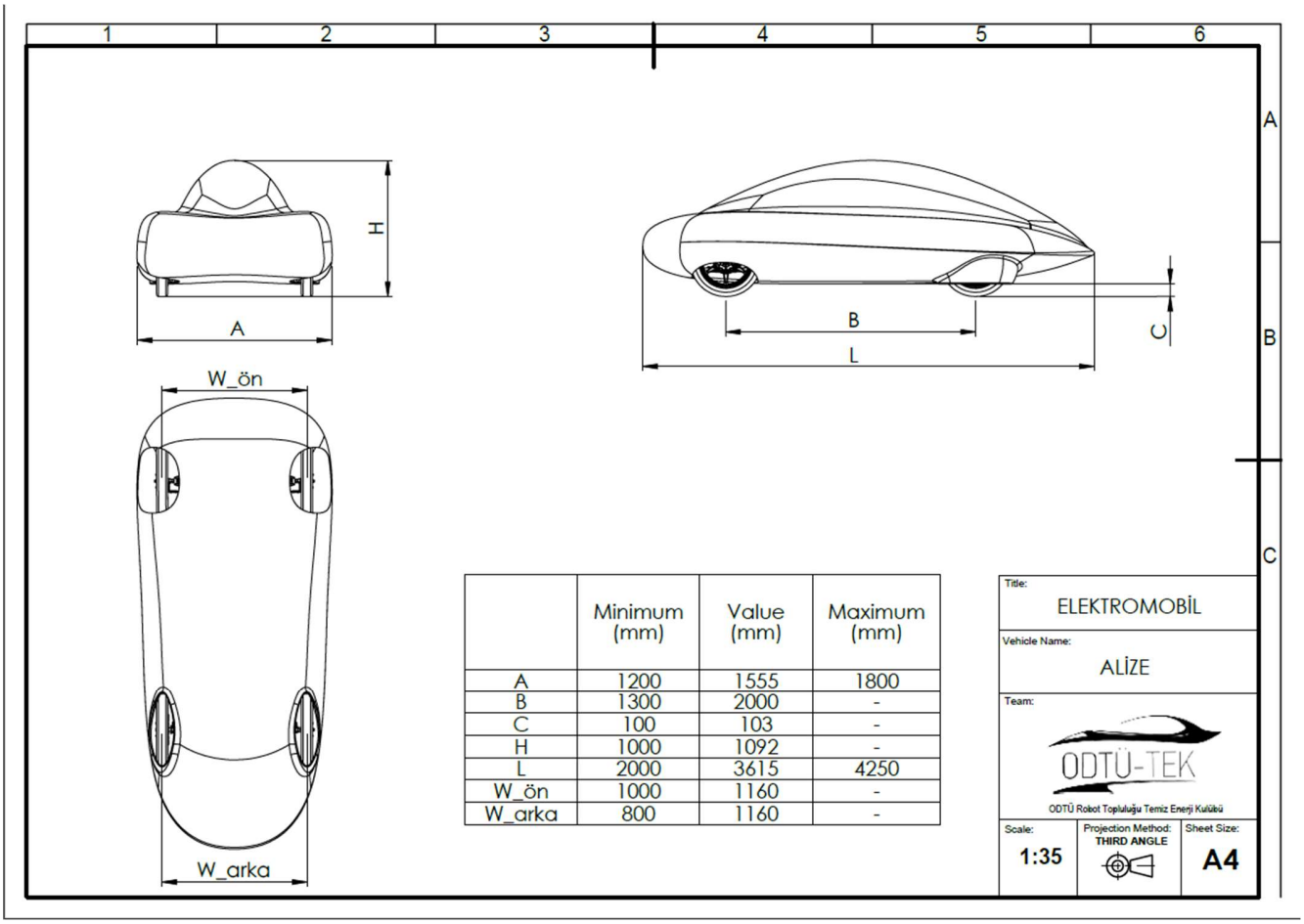

	Minimum (mm)	Value (mm)	Maximum (mm)
A	1200	1555	1800
B	1300	2000	-
C	100	103	-
H	1000	1092	-
L	2000	3615	4250
W_ön	1000	1160	-
W_arka	800	1160	-

Title: ELEKTROMOBİL
Vehicle Name: ALİZE
Team: ODTÜ-TEK
ODTÜ Robot Topluluğu Temiz Enerji Kulübü
Scale: 1:35
Projection Method: THIRD ANGLE
Sheet Size: A4

B. Aerodynamic Concerns for the Car

To concern aerodynamic characteristic of the car, first, we should know that "Aerodynamic Drag Force" is an important factor for efficiency; and this force can be calculated by using the following formula.

$$D = \frac{1}{2} \cdot \rho \cdot V^2 \cdot S \cdot C_D$$

Some of the parameters in this equation are constant () or more important for any other cases (), so the two important factors which affect the value of drag force are (drag coefficient) and (surface area). Therefore, inducing both of them is the best choice to get the minimum value of the drag force.

In the design process of the car, the chassis sizes and the general maximum measurements in the rules are limiting factors, so the process was started by concerning these. Secondly, the cabinet part (thick airfoil) and the rear wrapping part (low, symmetric airfoil) are designed in 2-D, separately, and combined in 3-D drawing. After that, to reduce the vortex generated by rear wheels, the back covers were made for each one.

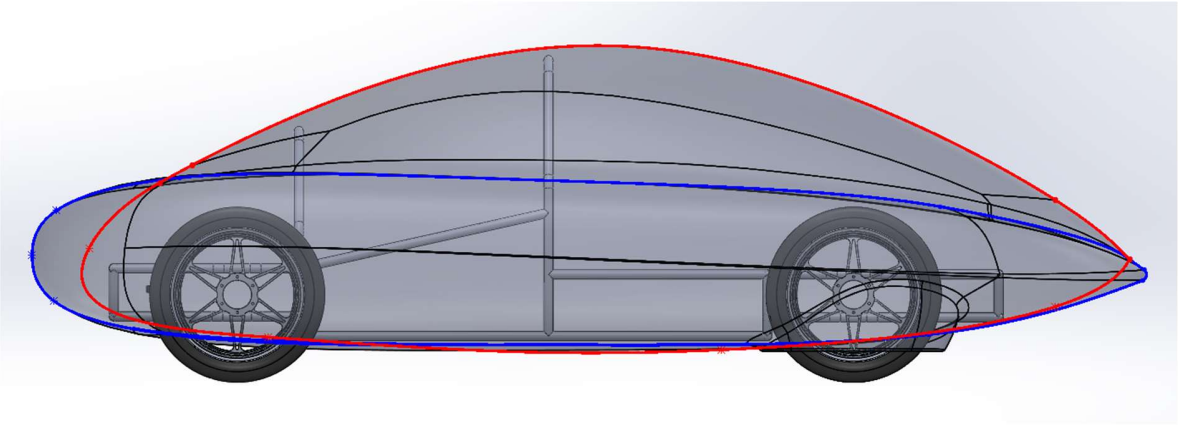

After making conceptual design, by using 4 different flow analysis software and their results, small changes were made. Finally, the results show that

$$L \cong -53.18\ N\ ,\ D \cong 14.53\ N$$

$$C_L \cong -0.02958\ ,\ C_D \cong 0.08948$$

Here is the pressure distribution for the car:

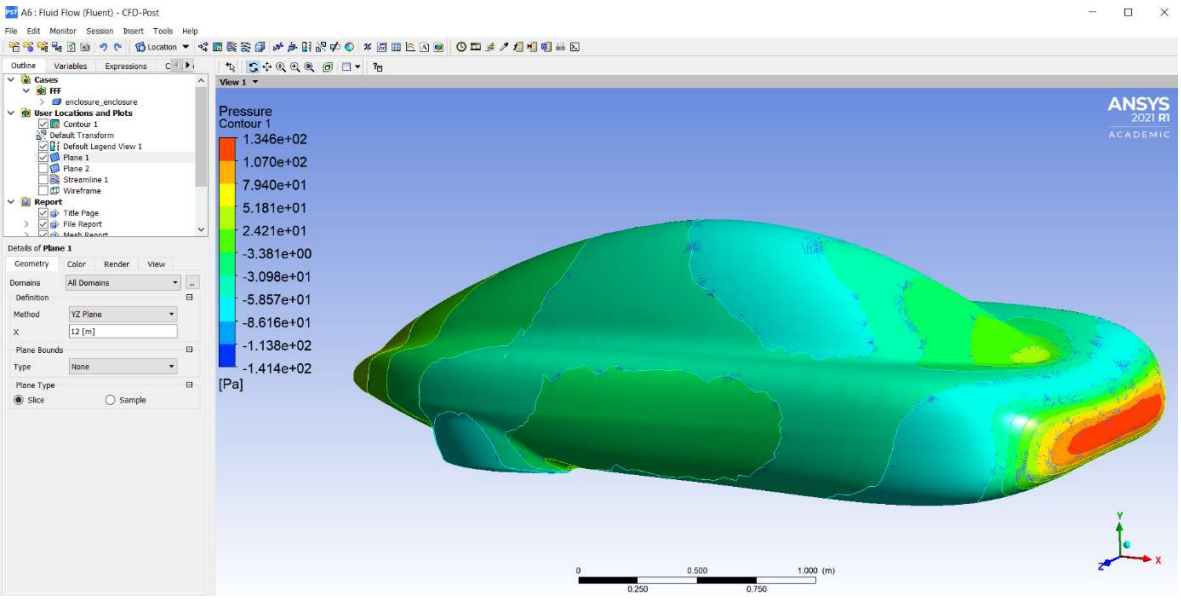

Here are the streamlines of the air outside of the car:

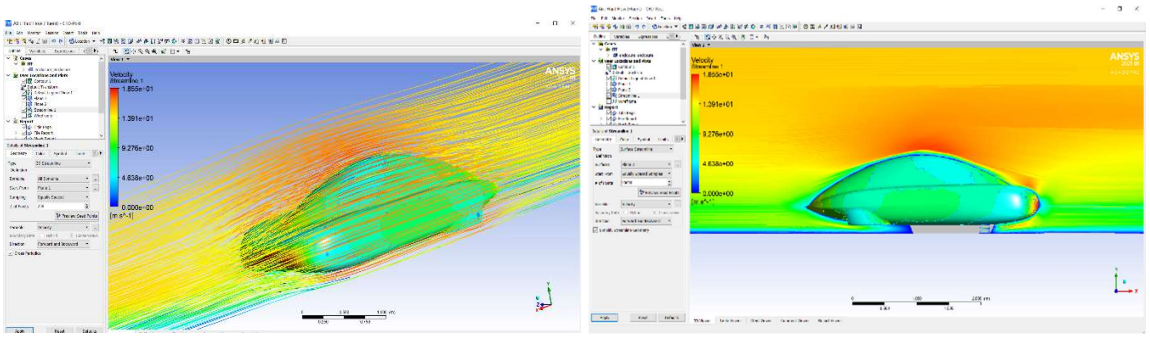

C.Manufacturing the Shell

After flow analysis and design were done by our team, the male model of our shell was produced from styrofoam using a 3 Axis started working to produce fiberglass mold. Firstly, Gel Coat layer is applied to our Styrofoam model to obtain a smooth surface. Shell manufacturing processes are listed down below.

1)Applying surface hardener to styrofoam model

2) Applying the polyester paste to certain areas in the surface and sanding.

3)Covering the model with Gel Coat

4) Laying up fabric to produce a female composite mold made of fiberglass by hand lay-up process.

5) Producing two female molds, top and bottom.

6) Assigning the areas of windows in female mold and placing cores.

7) Laying carbon fiber fabrics.

8) Producing the shell by process of applying resin to carbon fiber fabric then vacuuming the excess resin.

9) Trimming the shell and preparing the final product.

10)Assembling the carbon fiber shell and the chassis.

Pictures of the manufacturing process are listed;

Figure 18: styrofoam male model of Alize

Figure 19: Applying gel coat to model

Figure 20: Female composite mold

Figure 21: Laying carbon fiber fabric to mold

Figure 5: Top and bottom composite molds

Figure 6: Bottom shell after strengthened by cores

D. Energy Consumption Calculations

d.1 – "The time for the vehicle to travel 4000m at 50 kph."

"Mass"
$m := 220\ kg$

"Density of air"
$d := 1.225\ \frac{kg}{m^3}$

"Frontal surface area"
$A := 1.223\ m^2$

"Drag coefficient"
$Cd := 0.2$

"Coefficient of rolling res."
$Crr := 0.008$

"Angle of slope"
$\theta := 0\ deg$

"Acceleration"
$a := 0\ \frac{m}{s^2}$

"Efficiency of motor-drive system"
$eff := 0.9$

"Speed"
$v := 50\ kph = 13.889\ \frac{m}{s}$

$r\_wheel := \frac{0.55}{2}\ m$ "Radius of the wheel"

"Weight"
$W := m \cdot g = (2.157 \cdot 10^3)\ N$

$Ploss := 50\ W$ "Parasitic power loss due to bearings"

Road
$x := 4000\ m$

$Fdrag := \frac{1}{2} \cdot d \cdot Cd \cdot A \cdot v^2 = 28.9\ N$ "Force due to pressure drag"

$Frr := Crr \cdot W \cdot \cos(\theta) = 17.26\ N$ "Force due to rolling resistance"

$Fg := W \cdot \sin(\theta) = 0\ N$ "Force due to gravitational field"

$F\_a := m \cdot a = 0\ N$ "Force due to acceleration"

$Ftotal := Fg + Frr + Fdrag + F\_a = 46.16\ N$

$Ftotal \cdot x = (1.846 \cdot 10^5)\ J$

d.2 – " Power needed to reach 50 kph on a hill with %6 slope."

$Ftotal \cdot v = 641.107\ W$

d.3 – " Maximum velocity reached with a 1.5 kW motor on a hill with %6 slope."

"Motor Power"

$$P\_motor := 1.5\ kW$$

"Angle of slope"

$$\theta 2 := \operatorname{atan}(0.06) = 3.434\ deg$$

$$Fdrag := \frac{1}{2} \cdot d \cdot Cd \cdot A \cdot v^2 = 28.9\ N$$ "Force due to pressure drag"

$$Frr := Crr \cdot W \cdot \cos(\theta 2) = 17.229\ N$$ "Force due to rolling resistance"

$$Fg := W \cdot \sin(\theta 2) = 129.215\ N$$ "Force due to gravitational field"

$$F\_a := m \cdot a = 0\ N$$ "Force due to acceleration"

$$Ftotal2 := Fg + Frr + Fdrag + F\_a = 175.344\ N$$

$$v\_needed := \frac{P\_motor}{Ftotal2} = 30.797\ kph$$

15. Vehicle Electrical Schematic

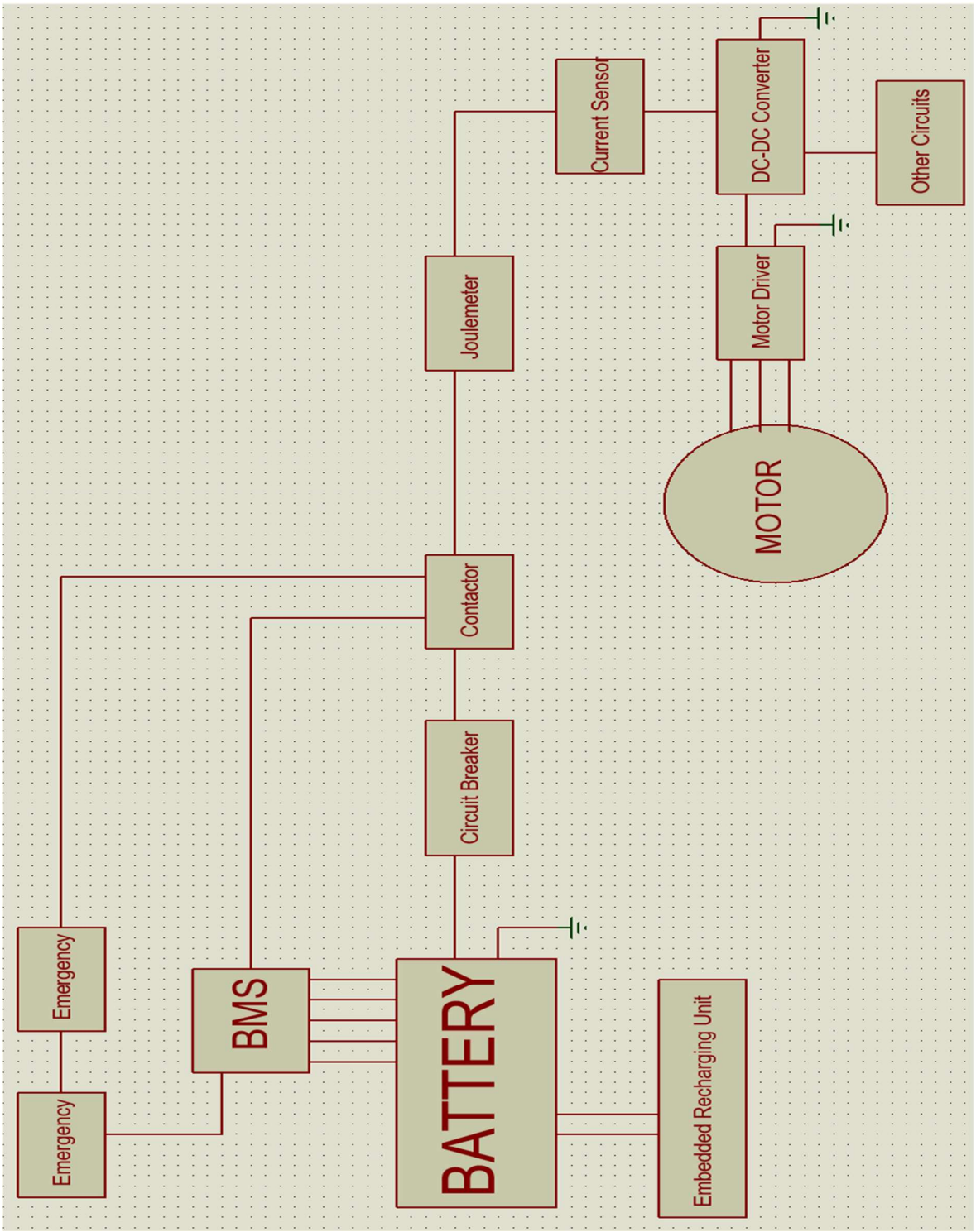

*Communication lines are not shown. Cable counts and width are not completely realistic.